Site Amplification Measurements for Ontario Seismic Stations Based on Ground Motion Relations and Horizontal to Vertical Ratios

by

Aaron J. Snider

A thesis submitted to the Faculty of Science

in partial fulfillment of the requirements

for the degree of

Bachelor of Science

(Honours)

Department of Earth Sciences

Carleton University

Ottawa, Ontario

March, 2005

The undersigned herby recommend to the Faculty of Science acceptance of this thesis by Aaron Snider, in partial fulfillment of the requirements for the degree of Bachelor of Science (Honours):

-

Dr. Dariush Motazedian,
Thesis Supervisor

Dr. Claudia Schröder-Adams,
Chair, Department of Earth Sciences

Abstract

Many of Ontario POLARIS (Portable Observatories for Lithospheric Analysis and Research Investigating Seismicity) stations are situated on soft soils, which increase the amplitude of seismic ground motions. These stations, along with CNSN (Canadian National Seismic Network) sites have provided recordings of fifty-four small to moderate earthquakes from which an initial measurement of site effects can be made based on two methods: a) comparison to the regional ground model, and b) horizontal-to-vertical ratios.

The time-series data from southern Ontario and western Quebec rock sites have been processed to produce Fourier acceleration amplitudes for a broad frequency range (0.2 – 20Hz), which were then fit to an existing ground motion model for eastern North America (Atkinson, 2004). The observed amplitudes show higher than predicted values at high frequencies. In addition, the eastern North America relation tends to over-predict amplitudes at small hypocentral distances and under-predict values at larger distances in south-central and southwestern Ontario, possibly due in part to a crustal waveguide effect.

Spectral plots of estimated site amplification were produced for each soil station by dividing the observed ground motion by that predicted by the modified regional relations, as well as by calculating horizontal-to-vertical ratios. Both methods showed comparable results, but the regional ground motion comparison generally showed higher amplitudes than the horizontal-to-vertical ratio technique. Estimates using both techniques showed good correlation with soil depths, with deep soil sites showing a clear fundamental frequency peak and high overall amplification. Fundamental frequency estimates from this study compare well with previous studies, although peak and average amplification values vary widely.

Acknowledgments

I would like to thank my supervisor, Dr. Dariush Motazedian, for his aid and encouragement. Much gratitude goes to Dr. Gail Atkinson for her guidance and instruction over the past three years, as well as for introducing me to seismology. I would also like to thank SanLinn Kaka and Curtis Brett for their help with the data processing, without which this work would not have been possible. Finally, many thanks to Jacqueline for her constant moral support and help during the last stages of writing.

Table of Contents

Table of Figures pg

1.0 Introduction

Thirty-one POLARIS (Portable Observatories for Lithospheric Analysis and Research Investigating Seismicity) seismograph stations have been deployed over the last three years in southern Ontario, providing a denser coverage for earthquake research than was previously available.

The ground motion recorded at a seismic site is the convolution of path, site and source effects. It is of great importance to separate these effects in order to accurately model the ground motion for input into seismic hazard studies as well as for the implementation of applications such as earthquake magnitude calculations and ShakeMaps (see Kaka and Atkinson, 2004).

It is known that soft soils can increase the duration and amplitude of shaking in a narrow frequency band. Since many POLARIS stations are located on soil, site response is an important issue in the use of recorded earthquake time series from this network. In most settings, earthquake ground motions are amplified primarily by the top 20m to 30m of soil.

In this thesis, ground motions from approximately thirty recently recorded earthquakes (mN 2.5 – 5.6) are compared to ground motion relations for eastern North America. To characterize site response, two techniques are used. First, the Horizontal to Vertical Spectral Ratio (HVSR) technique of Lermo and Chávez-García (1993) is used. The second method applies a ground motion model for Ontario to stations located on soil and estimates the effect of the soil layer by examining the residuals between the recorded and the predicted amplitudes.

1.1 Thesis Objectives

There are three main objectives of this study:

1. Determine if ground motion in Ontario follows the regional eastern North America (ENA) trend by examining ground motions at stations located on competent bedrock and comparing to an existing regional relation. Modify the ENA model to account for differences.
2. Characterize site response spectra at each POLARIS station, particularly those located on overburden.
3. Compare two methods of site response estimation:
   a) Horizontal-to-Vertical Spectral Ratios.
   b) An empirical spectral comparison of observed ground motions to ground motions predicted by the modified regional model.

1.2 Background Theory

1.2.1 Recorded Ground motion

The amplitude of ground motion recorded by a seismograph can be modeled as a convolution of the source waveform with several transfer functions:

$$S(t) = E(t) * P(t) * R(t) * I(t) \qquad (1.1)$$

Where:

S(t) = recorded seismogram
E(t) = source waveform
P(t) = path effect
R(t) = local site-response
I(t) = instrument response of the seismometer and the digitizer

Convolution in the time domain becomes simple multiplication in the frequency domain:

$$S(f) = E(f) \cdot P(f) \cdot R(f) \cdot I(f) \qquad (1.2)$$

The separation of these four terms, particularly the path and site terms, is an important issue in seismology.

1.2.2 Instrument Response

Instrument response is usually well defined within a certain frequency range for a properly calibrated system. The effect of instrumentation should be removed from recorded time series which can be done in both frequency and time domains. The broadband seismometers used in this study have a flat response spectrum between 0.1 to 8-10 Hz, beyond which reliability starts to decline. For consistency with past studies, ground motions are plotted from 0.2 to 20Hz, although statistics are compiled only for frequencies between 0.5 and 16Hz.

1.2.3 Path Effects

There are several path attributes which affect a seismic wave traveling through the crust. Firstly, geometric spreading is a result of conservation of energy over an expanding wavefront. Anelastic attenuation is due to scattering and absorption of the seismic wave and is inversely proportional to the ‘quality factor’, Q. Other factors include waveguide effects due to crustal structure, and the dominance of the various wave types (Atkinson, 2004). There are also directional effects due to crustal structure. Due to regional differences in crustal structure, attenuation of ground motion varies widely between different regions. For example, it is well known that amplitudes in eastern North America decay much less rapidly than in California.

1.2.4 Estimation of Source and Path effects

To simplify equation 1.2, the site effect is often assumed to be negligible ($S(f)= 1$) for hard rock sites, although several studies have shown that some amplification may still be observed (Siddiqi and Atkinson, 2002; Boore and Joyner, 1997).

Through regression analysis of an extensive database of ground motions, recorded over a wide range of hypocentral distances, the path and source parameters can be empirically estimated (Atkinson and Mereu 1992, Atkinson 2004).

1.2.5 Site Effects

Being able to characterize the site response term is critical to estimating the amplitude of ground motion for a particular area or location. Soils have lower density and shear wave velocity than rocks. Seismic impedance of soil, which is the product of density (ρ) and shear wave velocity (V_S) is less than the seismic impedance of rock. When a seismic wave reaches a soft soil layer, its duration and amplitude within a narrow frequency band are changed due to changes in seismic impedance of the medium and conservation of momentum. Quantitatively, the energy of an S-wave is $E = 2\pi^2\rho V_S f A^2$, where f is frequency, and A is the amplitude of the wave. Thus, when a wave passes from a material of low impedance to a material of high impedance, the amplification increases by conservation of energy:

$$A_1/A_2 = (\rho_2 V_{S2} / \rho_1 V_{S1})^{1/2} \qquad (1.3)$$

(Boore and Joyner, 1997)

A common method of characterizing local amplification effects for engineering and seismological studies is the National Earthquake Hazard Reduction Program (NEHRP) classification scheme, which categorizes sites based on the average shear wave velocity of the top thirty metres. However, this requires a velocity profile down to thirty metres, or detailed knowledge of the subsurface material. Since these details are available for only a few sites in this study, this site classification scheme will not be discussed further. Shear-wave velocity profiles for several POLARIS sites are available in Beresnev and Atkinson (1997) and Murphy (2003).

Resonance effects are due to a matching between the natural frequency of the soil and the frequency content of seismic wave and constructive interference caused by the trapping of waves between two layers of different properties. The constructive effect occurs at the fundamental frequency, f_0, as well as at higher harmonics, f_n, although these higher modes are not always observed. These resonant frequencies are dependent on the shear wave velocity and the thickness of the layer (z):

$$f_n = (2n-1)V_S / 4z \,. \qquad (1.4)$$

The amplification observed at the fundamental frequency is estimated by Joyner and Boore (1981) as the ratio between the seismic impedance of the soil and bedrock layers.

In addition, local topography, both at the surface and at the bedrock-soil interface can add complexity to the site transfer function, through focusing, splitting and redirection of incident waves (Bard, 1994).

1.3 Estimation of Site Amplification

Numerous techniques have been proposed to estimate the near-surface site amplification. The most common methods are summarized as follows:

Numerical approach: Shear wave velocity and density of each layer, as estimated from either seismic refraction studies or borehole measurements, can be input into numerical modeling software to produce theoretical amplification spectra (Beresnev and Atkinson 1997; Boore 1996, 1997; Murphy 2003). For this method to give a reliable estimate of the amplification, the properties of the subsurface must be well known. Thus, this method is expensive and labour-intensive, but effectively estimates the fundamental frequency and possibly the amplification for relatively simple subsurface conditions.

Standard Spectral Ratios (SSR): Observed ground motion from the site in question is divided by the observed ground motion from a nearby reference site which is assumed to experience no amplification. The path term is assumed to be the same at both stations, and thus the remaining spectrum consists of only the site response. The usefulness of this technique depends on the availability of a nearby rock station (Field and Jacob, 1995). Consequently, extensive overburden cover in southern Ontario and wide spacing between seismograph sites limits the use of this technique at most soil stations.

Horizontal to Vertical Spectral Ratios (HVSR): The Horizontal to Vertical technique is a modification of the method proposed by Nakamura (1989) for use with microtremor measurements. The shear window of shaking of the horizontal component is divided by that of the vertical component, with the common assumption that the vertical component is devoid of any near-surface amplification effects. Thus the site effect term is isolated in the resulting spectrum (Lermo and Chávez-García, 1993). While it is widely accepted that this method successfully estimates the fundamental frequency, its determination of the amplification factor is controversial (Field and Jacob, 1995).

As an alternative to the above methods, the amplification may be inferred from comparison with a regional attenuation model. A similar method is used by Atkinson and Cassidy (2000) to estimate site amplification at soil sites in the Fraser Valley, British Columbia. Observed ground motion is divided by the predicted ground motion from a regional attenuation model based on ground motion recorded at rock stations. The rock stations are assumed to experience no site effect. If the source and path effects for a region are well known, then this method may successfully estimate the site amplification.

1.4 The Seismograph Array and the Study Region.

The POLARIS seismograph array consists of thirty-one stations in Ontario, and are an important addition to the eleven existing Canadian National Seismograph Network (CNSN) sites, enabling a denser coverage for local seismicity studies as well as more accurate seismic hazard models for engineering applications. These stations are shown in Figures 1.1 and 1.2.

However, many of the installed stations are of limited use for these applications since they are installed on soft soils. Ontario has been extensively glaciated, and much of the province is covered by thick quaternary tills. Precambrian bedrock exists in the north and east of the study area, while Paleozoic layers of limestone and shale overlie the crystalline basement in central and southwestern Ontario, where much of the exposed Paleozoic bedrock is highly weathered. The station locations and the generalized surficial geology are tabulated in Tables 1.1 and 1.2. Because of the highly variable surficial geology, there is a wide range of site responses observed at POLARIS stations. Existing CNSN stations are all located on competent bedrock, and exhibit minimal amplification due to site effects. (Siddiqqi and Atkinson, 2002)

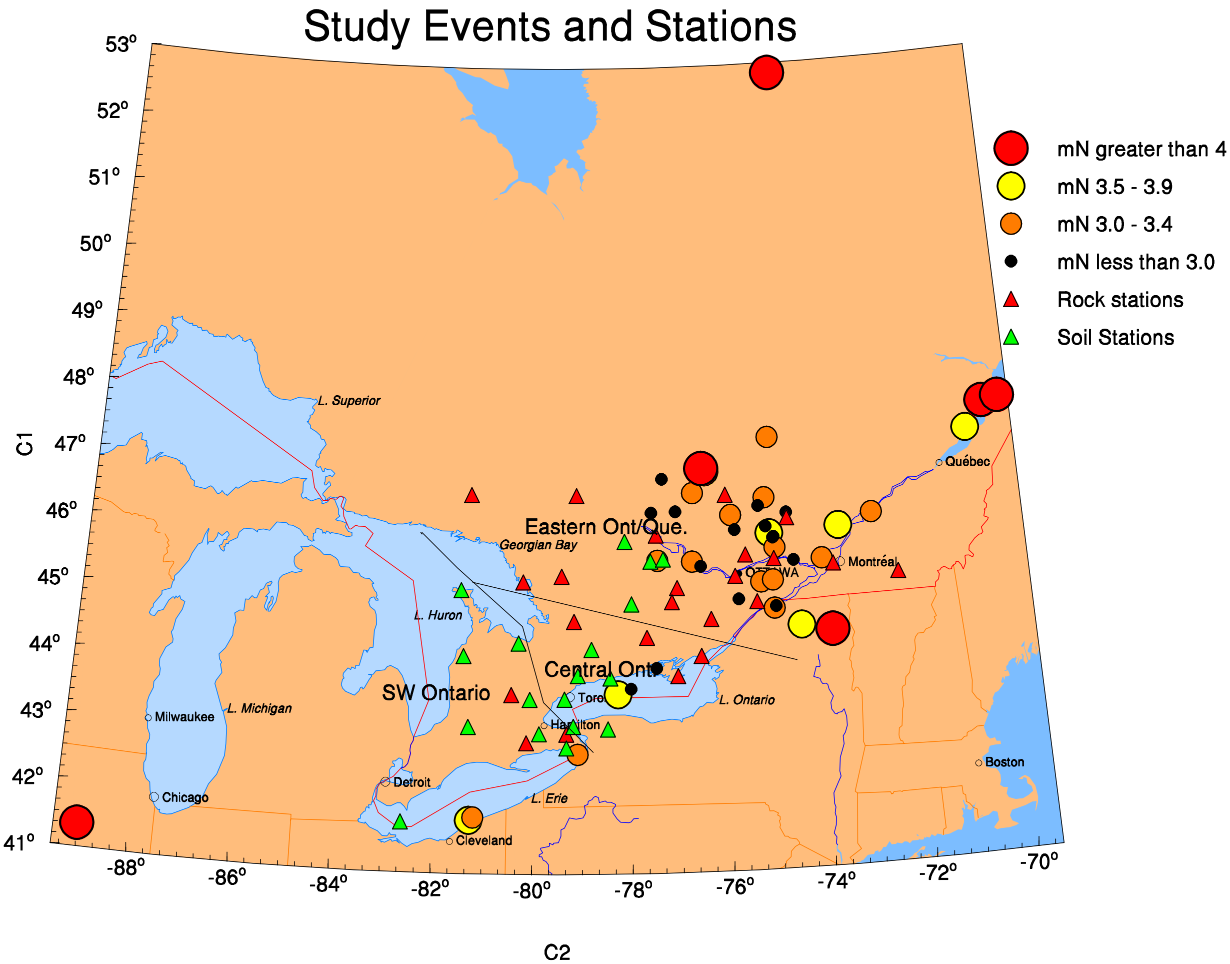

Figure 1.1: Stations and events used in study. Several events occur at the same location, and thus the symbols are indistinguishable from previous events.

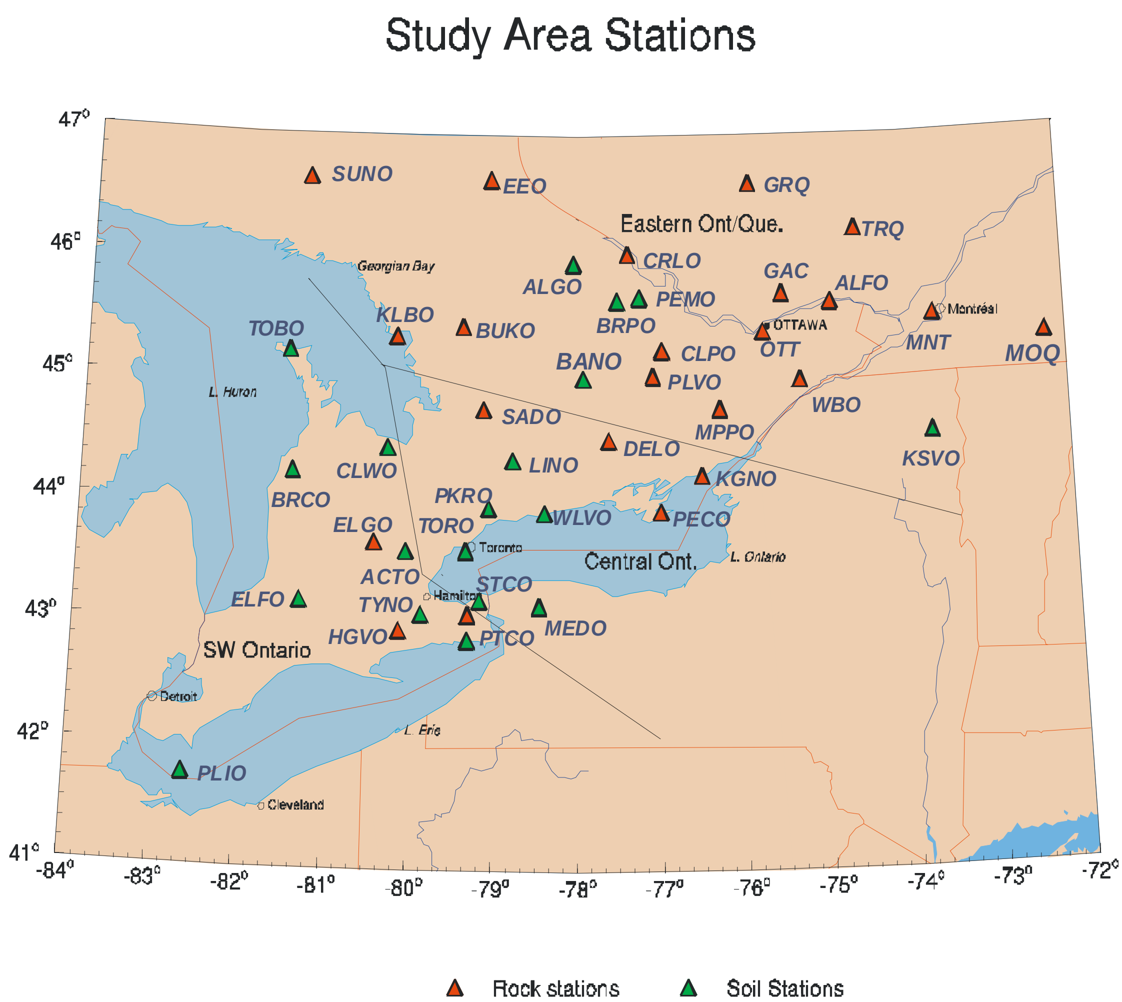

Figure 2.2: POLARIS and CNSN stations in the study area.

Station	Region	Latitude	Longitude	Regional Surficial Geology	Field observations by author
ACTO	Southwest	43.608	-80.062	till moraine	
ALGO	East	45.954	-78.05	Spillway	Local geology: sand, possibly some man-made fill. Topography: located at top of 30m hill.
BANO	East	45.02	-77.93	Shallow till/rock ridges	Local geology: till, rock outcrops within 100 m of station. Topography: rough.
BRCO	Southwest	44.244	-81.442	till plain-undrumlinized	
BRPO	East	45.651	-77.51	Sand plain	Local geology: sand Topography: flat.
CLWO	Southwest	44.449	-80.301	till plain / escarpment	Local geology: soil. Topography: Located on top of Niagara Escarpment. Escarpment face is approximately 500m from site.
ELGO	Southwest	43.676	-80.44	till plain – drumlinized	**seismometer located on weathered Paleozoic bedrock (Murphy, 2003)*
HGVO	Southwest	42.961	-80.13	clay plain	**seismometer located on weathered Paleozoic bedrock (Murphy, 2003)*
KSVO	East	44.552	-73.68		Local geology: glacial till, Crystalline rock outcrops in region Topography: Rough. Located at top of 40m slope, which dips west.
LINO	Central	44.354	-78.78	till plain – drumlinized	Local geology: till/soil plain. Outcropping limestone bedrock in region (~3km north of site) Topography: flat
MEDO	Central	43.165	-78.455		
PEMO	East	45.677	-77.24	shallow till / rock ridges	Local geology: located on till, bedrock outcrop 20m from site. Topography: rough. From site owner: subsurface bedrock topography dips steeply under site.
PKRO	Central	43.963	-79.07	till plain – drumlinized	
PLIO		41.751	-82.628	beveled till plain	
STCO	Central	43.208	-79.17	sand plain	
TORO	Central	43.614	-79.343	landfill on beach deposits	
TOBO	Southwest	45.226	-81.523		Geology: located on till, Paleozoic dolostone outcrop 3m from seismometer. Topography: flat. Bedrock topography unknown; high bluffs of the Niagara escarpment approximately 5km away.
TYNO	Southwest	43.094	-79.87	clay plain	
WLVO	Central	43.923	-78.397	till plain - drumlinized	

Table 1.1: Site locations, regional surficial geology (Chapman and Putnam, 1984), and field observations for soil stations in the study area.

Station	Region	Latitude	Longitude	Field Observations by Author
ALFO	East	45.628	-74.88	
BUKO	East	45.442	-79.399	
CLPO	East	45.246	-76.96	
CRLO	East	46.037	-77.38	
DELO	Central	44.518	-77.62	
EEO	East	46.641	-79.073	
GAC	East	45.703	-75.478	
GRQ	East	46.607	-75.86	
KLBO	East	45.356	-80.213	Geology: Precambrian bedrock outcrop. Topography: at summit of 30m hill
KGNO	Central	44.227	-76.49	
MNT	East	45.502	-73.623	
MOQ	East	45.312	-72.254	
MPPO	East	44.77	-76.26	Geology: Precambrian bedrock outcrop. Topography: surface topography is flat, bedrock topography unknown.
OTT	East	45.394	-75.717	
PECO	Central	43.934	-76.99	Local geology: weathered limestone, covered by thin (<30cm) till. Seismometer located on bedrock. Topography: flat, 50m bluffs located ~500m away.
PLVO	East	45.04	-77.075	
PTCO	Southwest	42.884	-79.31	
SADO	Central	44.769	-79.142	
SUNO	East	46.644	-81.344	Geology: Precambrian bedrock outcrop. Topography: roughly flat at site, but rough in local region.
TRQ	East	46.222	-74.556	
WBO	East	45	-75.275	

Table 1.2: locations and field observations for rock stations within the study area. CNSN stations are italicized

2.0 Database for Analysis and Processing

A total of 1028 records from fifty-four small to moderate earthquakes that occurred between January 2002 and December 2004 were processed, as well as one which occurred on March 6, 2005. The Nuttli magnitude, mN, and location for these earthquakes were found by Earthquakes Canada and posted to their database at www.earthquakescanada.ca. The recorded seismograms at each station in the study area were downloaded periodically using the Geologic Survey of Canada's Automatic Data Request Manager (Autodrm) at ftp.seismo.nrcan.gc.ca. The seismograph data was then decompressed and the time series data was plotted using the software Geotool. The shear wave window of strongest shaking was selected, as well as a pre-event noise window, normalized to the duration of the shear window. Figure 2.1 shows the shear and noise window selections for time-series data of the March 6, 2005 Charlevoix (mN 5.4) event recorded at station KLBO.

The Fast Fourier Transform algorithm (Cooley and Tukey, 1965) was then used to compute the frequency spectrum of the shear and noise windows. This was done using the FORTRAN software, AGRAM, written by Gail Atkinson. A five percent taper was applied at each end of the time series before the transformation. The resulting Fourier spectrum was smoothed and tabulated into frequency bins of 0.1 logarithmic units, over the frequency range 0.1 to 20Hz.

Several Fortran and C programs were written or modified to manipulate the database. The main goals of the software were to exclude unreliable data, parse the data into a format readable by spreadsheet programs and other software, and to sort and find specific data.

Two criteria were used to eliminate unreliable data. First, only Fourier amplitudes with a minimum signal to noise ratio of 2 were retained. Secondly, below a certain level of ground motion, amplitudes are not reliably recorded by the instrument, regardless of the signal to noise ratio (Atkinson 2004a), so only data within the magnitude-distance requirements listed in table 2.1 were retained:

Nuttli Magnitude	Maximum hypocentral distance [km]	
	frequency < 1Hz	frequency > 1Hz
$2.5 \leq mN < 3$	0	100
$3 \leq mN < 3.5$	80	200
$3.5 \leq mN < 4.0$	100	400
$4 \leq mN < 4.5$	200	800
$MN \geq 4.5$	800	2000

Table 2.1: Magnitude-distance requirements for the study dataset. (after Atkinson 2004)

After the above requirements were applied, the remaining Fourier amplitudes were output to a single file for further sorting and manipulation. Appendix A contains a flowchart displaying the connection between this database and the subsets used throughout this study.

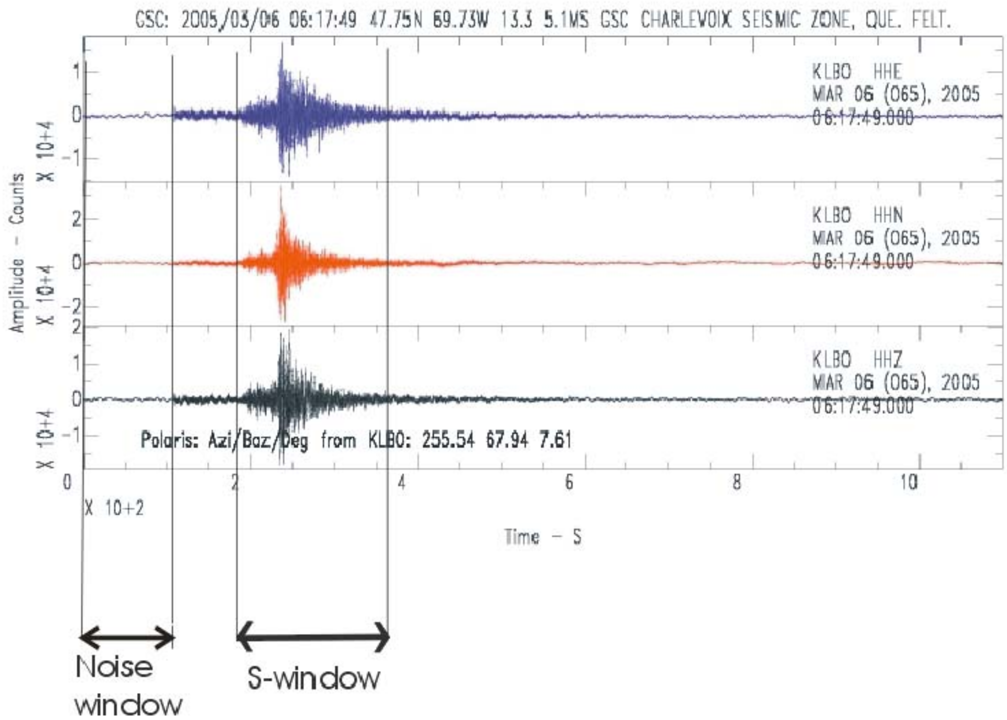

Figure 2.1: Example of time series data for Charlevoix mN 5.4 event, recorded at station KLBO. Noise and shear windows are indicated. In order to calculate the signal-to-noise ratio, the noise window is normalized to the size of the S-window.

3.0 Methods

In this section, the method used to compare ground motion in the study area to the eastern North America trend is examined, then the HVSR method of estimating site amplification is discussed. Finally, the use of the regional ground motion relations to estimate response at soil sites is presented.

3.1 Observed Ground Motion Compared to Eastern North America Trend

The POLARIS and CNSN arrays have provided a database of 1028 ground motion records for Ontario. This database is compared to the general ground motion trend for eastern North America; in particular, the empirical relation tabulated by Atkinson (2004). The 2004 relation is similar to the commonly used Atkinson and Mereu (1992) attenuation model, but was determined from a larger ground motion database. While the Ontario/Québec database is not large enough to use a new regression analysis to determine a local attenuation model, the data can be fit to the previous relation.

Atkinson performs a maximum-likelihood regression on the vertical component of motion of recorded data from across eastern Canada and the United States. This resulted in the following 'hinged-trilinear' model for ground motion amplitudes:

$$\log A = c_1 + c_2(m1-4) + c_3(m1-4)^2 - 1.3\log R - c_4 R \qquad \text{for } R<70\text{km} \qquad (3.1a)$$

$$\log A = c_1 + c_2(m1-4) + c_3(m1-4)^2 - 1.3\log(70) + 0.2\log(R/70) - c_4 R \qquad \text{for } 70<R<140\text{km} \qquad (3.1b)$$

$$\log A = c_1 + c_2(m1-4) + c_3(m1-4)^2 - 1.3\log(70) + 0.2\log(140/70) - 0.5\log(R/140) - c_4 R \qquad \text{for } R>140\text{km} \qquad (3.1c)$$

A: predicted Fourier acceleration amplitude in cm/s.
c_1, c_2, c_3, c_4: regression coefficients (frequency dependent).
R: hypocentral distance in km.
m1: empirical estimate of moment magnitude, from Chen and Atkinson (2002).

In Equation 3.1, geometric spreading is characterized by the factors -1.3, +0.2, and -0.5. Anelastic attenuation is represented by the coefficient c4. A plot of the predicted ground motion from the above model is shown in Figure 3.1 along with observed ground motion from this study for twenty earthquakes $3.0 \leq mN \leq 3.5$.

In this study, Equation 3.1 is used to determine predicted Fourier amplitudes for all records in the database. To do this, the m1 value had to be determined for events not previously used by Atkinson (2004). (ie. events after December 2002) Chen and Atkinson (2002) define m1 as:

$$m1 = 4.4665 + 0.7817\log(A_1)_{10} + 0.1399(\log(A_1)_{10})^2 + 0.0351(\log(A_1)_{10})^3 \qquad (3.2)$$

Where, $(A_1)_{10}$ is the 1Hz predicted Fourier acceleration at a distance of 10km.

To determine $(A_1)_{10}$, equation 3.1 is first manipulated to find the source spectra, A_{src}:

$$\log A_{src} = \log A + 1.3\log R + c4R \text{ for } R<70\text{km},$$

$$\text{(and similarly for } 70<R<140\text{km and } R>140\text{km)} \qquad (3.3)$$

Then the source amplitude is attenuated to a reference distance of 10km using Equation 3.1.

In order to prevent site amplification from biasing the magnitude estimate, rock sites from POLARIS and CNSN arrays in eastern Canada are used to find m1, following the same magnitude-distance requirements noted in Section 2.

The use of m1 has advantages over other magnitude scales since moment magnitudes are determined for very few of the study events, and unlike various other magnitude scales, it is based on the amplitude of ground shaking in a clearly defined frequency range (Atkinson 2004).

A C program was written to determine m1 for each event. This program calculates m1 from Equations 3.2 and 3.3, then averages the estimates from every rock station in the database that meet the magnitude-distance requirements listed in Table 2.1. For this study, events with fewer than three m1 estimates were eliminated from the database, reducing the database to thirty events.

The database was then sorted into four subsets: rock stations, vertical component; rock stations horizontal components; soil stations, vertical component; and soil stations, horizontal components. The vertical and horizontal components are treated separately throughout the entire study.

The fit of the study data to the eastern North America model (Equation 3.1) is then characterized by examining the residuals between the observed and modeled ground Fourier acceleration (Faccn):

log(residual) = log(observed Faccn) – log(predicted Faccn)

If the Ontario data fits the eastern North America model the residuals should plot close to unity, and show no trends with distance or frequency. An attempt will be made to explain any obvious trends, and a correction factor will be applied to account for this in the next chapter.

Thus, once a relation is found that acceptably models the ground motion at rock sites within the study area, deviance from this trend of observed ground motion at soil sites could be attributed to site response, if the site effect term at rock stations is assumed to be close to unity.

Fit of 1Hz Ontario data to GMA04 trend for ENA - m1=3.25 +/-0.25

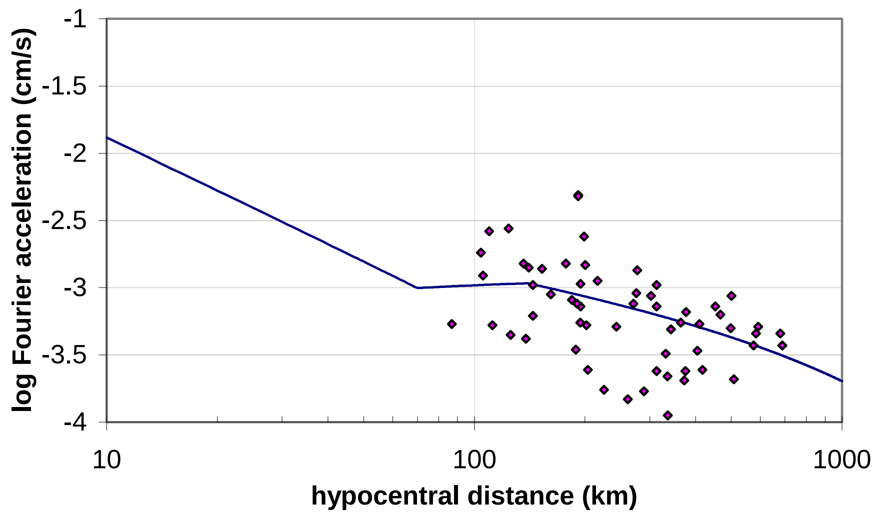

Fit of 5Hz Ontario data to GMA04 trend for ENA - m1=3.25 +/-0.25

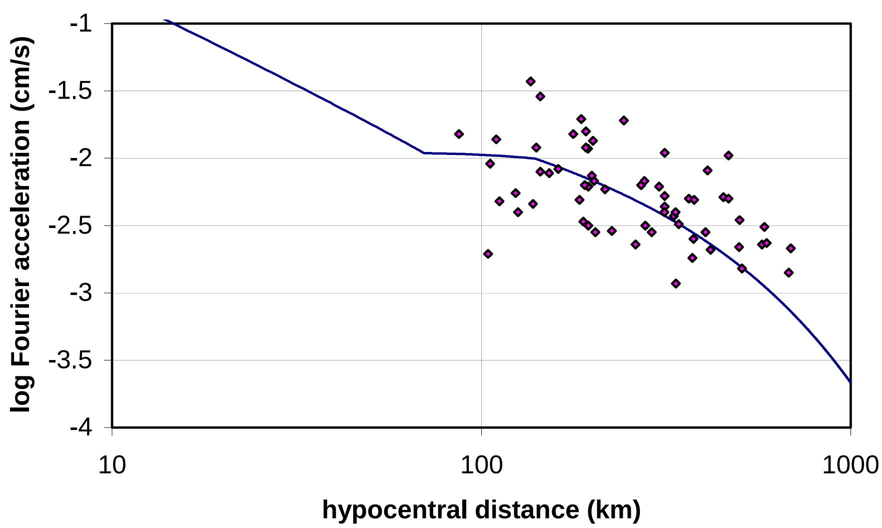

Figure 3.1: GMA04 Ground motion model for Eastern North America (ENA) for 1Hz and 5Hz, from Atkinson (2004). Diamonds represent observed Fourier acceleration in cm/s from 20 events 3.0<mN<3.5 at POLARIS and CNSN stations in the study area.

3.2 Using Horizontal - Vertical Spectral Ratio to Estimate Site Amplification

3.2.1 Introduction

As its name implies, the Horizontal to Vertical Spectral Ratio method involves dividing the frequency spectrum of the horizontal component of shaking by that of the "reference" vertical component.

This technique is similar to the receiver-function technique, used in teleseismic studies to determine the velocity structure of the crust (Langston, 1979). Since Nakamura (1989) first applied this technique to microtremor measurements to examine the local effect of soft soils, this form of site response estimation has been widely applied. It has been extensively demonstrated that for simple topography, the vertical component is relatively insensitive to near-surface amplification compared to the horizontal components. However, this is not necessarily the case for localities with two-dimensional topography such as sedimentary basins, where focusing and reflection of seismic waves occur (Al Yuncha and Luzón, 2000).

Lermo and Chávez-García (1993) modify this technique for use with the high amplitude shear-wave part of earthquake records. They suggest that the tendency of the raypath to refract towards the vertical within soft soils counterbalances any amplification of the vertical component, since particle motion in S-waves is tangential to the propagation direction. Furthermore, from analogy with teleseismic studies, the horizontal component contains P-S wave conversions due to local structural discontinuities, while the vertical component is relatively uninfluenced (Field and Jacob, 1995).

Although the physics is not clearly understood, it has been demonstrated that this simple technique finds the fundamental mode frequency of strongest shaking, and provides a rough estimate of peak amplification (Bard 1994, Murphy and Eaton 2005, Molnar *et al.,* 2004).

3.2.2 Method

The horizontal-to-vertical spectral ratio (HVSR) technique of Lermo and Chávez-García (1993) is applied to the same ground motion database used for the Ontario ground motion study. However, the database is larger since it was not necessary to find m1 for an event in order to include it. Only records that had a signal-to-noise ratio greater than two and met the magnitude-distance requirements from Table 2.1 were retained.

A C program was written to find the H/V ratios for each event. With the formatted and reduced Fourier amplitude database as the input, the HVSR was found for each event recorded at a particular station. Then, the individual spectra were averaged, the standard deviation and 90% confidence interval were determined for each frequency bin. Finally, the peak amplitude, the frequency of the peak amplitude (fundamental mode frequency) and average amplification between 0.5 and 16Hz were computed.

Thus the HVSR was found for each station using:

$$S_{jk} = \frac{1}{N}\sum_{i=1}^{N}\frac{< H_{jik} >}{< V_{jik} >} \tag{3.4}$$

where S_{jk} is the ratio for the k^{th} frequency bin at the j^{th} station, averaged over N events. (Murphy and Eaton, 2005). The two horizontal components were treated as separate records. Individual files were output for each station and compiled using a spreadsheet program.

3.3 Using Regional Ground Motion Trend to Estimate Site Amplification

3.3.1 Introduction

The regional attenuation model can be used to predict amplitudes at soil sites, with the assumption that it accurately models path and source effects for the region. If the observed ground motion is divided by the predicted ground motion, source and path effects cancel, isolating the site term.

3.3.2 Methods

Once a regional ground motion model is characterized for Ontario, it can be used to predict Fourier amplitudes at the soil stations. Since most of the amplification is observed in the horizontal component, the observed horizontal component Fourier amplitudes are divided by the corresponding predicted horizontal Fourier amplitudes:

$$\log(\text{amplification}) = \log(\text{observed}_H) - \log(\text{predicted}_H)$$

The same can be done for the vertical component, although it is not done in this study. The same events that were used to determine the Ontario ground motion model were used to find the spectral amplifications at soil sites. 212 records were used, which gave between two and twenty-one amplification estimates per station.

A C program was written to find the spectral amplification functions for each record. The horizontal soil database was input, the predicted amplitudes were calculated for each event recorded at a particular station, and the individual spectra were averaged for each station. Finally the standard deviations and 90% confidence intervals were determined, and estimates of the peak amplitude, fundamental frequency and average amplification between 0.5 and 16Hz were calculated. Results for each station were then combined with the HVSR data in a spreadsheet program.

4.0 Results and Discussion

This section is organized as follows:

4.1 Comparison of ground motions observed in Ontario to the regional model;

4.2 Site response estimation for soil stations in the study area by using HVSR method;

4.3 Site response estimation using regional ground motion models by analysis of the residual distribution at soil stations in the study area, and comparison with HVSR results.

4.1 Observed Ground Motion Compared to Eastern North America Trend

Ground motions at rock sites

Residuals of Fourier acceleration amplitude are plotted against distance in Figures 4.1 and 4.2 for two frequencies (1Hz and 5Hz) representing a range important in engineering studies. For the vertical component,

$$\log(\text{residual}) = \log(\text{observed}) - GMA04_Z$$

where $GMA04_Z$ is the predicted Fourier amplitude for vertical component using Equation 3.1. The horizontal component was also examined for any distance trends, using:

$$\log(\text{residual}) = \log(\text{observed}) - GMA04_H$$

where, $GMA04_H = GMA04_z + [0.0234+0.106\log f]$

(Atkinson, 2004)

There are small trends with distance in Figures 4.1 and 4.2. A least-squares fit of the data shows that any trend is small relative to the error on the regression coefficients. To examine possible amplification at high frequencies, the residuals are plotted against frequency in Figure 4.3. A visible trend exists showing higher than predicted amplitudes at high frequencies, which can be modeled by a linear least squares fit of

log residual = -0.002 + 0.07logf for the vertical component, and

log residual = -0.01 + 0 08logf for the horizontal component.

The trends are similar for both components, suggesting this frequency dependence may not be a site effect, since the horizontal component would be expected to show more amplification. From the above analysis, the following equations model ground motions in southern Ontario and southwestern Québec.

$$GMA04_Z + [-0.002 + 0.07\log f] = ONT_Z \tag{4.1a}$$

$$GMA04_H + [-0.01 + 0.08\log f] = ONT_H = GMA\ 04_Z + [0.012 + 0.185\log f] \tag{4.1b}$$

Mean residuals from individual stations are plotted in Figure 4.4a,b and Figure 4.5a,b to check fit of the new ground motion relations for the study sites. Residuals were plotted using

log (residual) = log(observed) – ONT_Z for the vertical component, and

log (residual) = log(observed) – ONT_H for the horizontal.

All stations plotted within one standard deviation of unity, with the exception of KLBO and SUNO, which had small standard deviations due to the small number of records collected at these sites (three events each). Thus, it is concluded that although there is wide variability between the stations, it is not statistically significant.

Ground motions at soil sites

Observed ground motions from stations located on overburden are compared to ground motions predicted by Equations 4.1(a,b). Then the amplification of ground motion due to a soil layer can be characterized by the ratio between the observed ground motion at the surface and the predicted ground motion input at the base of the soil layer. Before examining individual soil spectra, the residuals are plotted against distance for 1Hz and 5Hz in Figures 4.6a,b and 4.7 a,b. where

$$\log(\text{residual}) = \log(\text{observed}) - ONT_Z \text{ , or}$$

$$\log(\text{residual}) = \log(\text{observed}) - ONT_H$$

The plots show a strong positive trend with distance. This is unexpected, since the residual plots from the rock sites did not show any distance dependence.

Examination of unexpected residual – distance trend

The soil database is heavily weighted with stations from southern Ontario. Since there are few rock stations in this region, this trend may be a regional phenomenon, independent of the type of site. To study this, the entire vertical component database (both rock and soil stations) is examined, using the original $GMA04_Z$ model.

Depth to Precambrian basement increases from the northeast to the southwest within southern Ontario (Boyce and Morris, 2002). Since much of the ground motion originates in western Québec, the increase in thickness of the Paleozoic layer may cause amplification to increase, due to both path and site effects. (D. Motazedian, pers. comm.) This hypothesis is examined by first separating the study database into three regions which roughly correspond to the bedrock geology of the study area, as shown in Figure 1.1 and summarized in Table 4.1.

Region	Geology	Stations
Eastern Ontario / Western Québec	Mainly glaciated Precambrian shield, as well as Ordovician limestone and shale of the Ottawa Embayment.	KLBO, BUKO, ALGO, PEMO, CLPO, KSVO, PLVO, BANO, MPPO, ALFO, SUNO, CRLO, EEO, GAC, GRQ, MNT, MOQ, OTT, TRQ, WBO
Central Ontario	Ordovician limestone and shale layers with thick glacial deposits throughout. Depth to Precambrian basement: ~0 to 500m	DELO, LINO, MEDO, PECO, PKRO, TORO, STCO, WLVO, KGNO, SADO
Southwestern Ontario	Silurian and Devonian limestone and shale, with thick glacial deposits throughout. Includes Niagara escarpment. Depth to Precambrian basement: ~500 to 1500m	ACTO, BRCO, CLWO, ELFO, HGVO, PLIO, PTCO, TOBO, TYNO

Table 4.1: Sub-regions of the study area, corresponding to Figure 1.1.

The 5Hz vertical component residuals in the three regions are plotted in Figures 4.8 a,b,c. There is no obvious trend with distance in eastern Ontario, although a trend may exist among the soil site data. In both central and southwestern Ontario, a strong amplitude distance trend exists. This suggests that the amplification is not purely a site effect.

The source regions are examined in Figures 4.9 and 4.10 to determine if the observed trends are visible in individual events. For the southern Ontario dataset, residuals generally plot well below zero for distances under 200km, and above zero at larger distances. However, when the individual sources are examined, no conclusive trend exists. The database is significantly influenced by several events, particularly in southern Ontario at distances closer than 200km and greater than 800km. At large distances, residuals from individual events are scattered over a wide range of amplitudes, and show no particular trend. The August 8, 2004 Port Hope event was well recorded across the entire network and shows mostly low residuals in southern Ontario at distances closer than 200km, and higher residuals beyond this point. The June 30, 2003 Lake Erie event may show a trend throughout the network, while the western Québec events do not show an obvious trend.

Since the sources of the majority of ground motions are oriented to the northeast of the study area, it is possible that the crustal structures of southern Ontario are producing a good waveguide along a northeast-southwest path. The June 28, 2004 Illinois event may support this hypothesis, as the source is oriented to the southwest of the study and shows high residuals. However, a larger database is needed to reach a definitive conclusion.

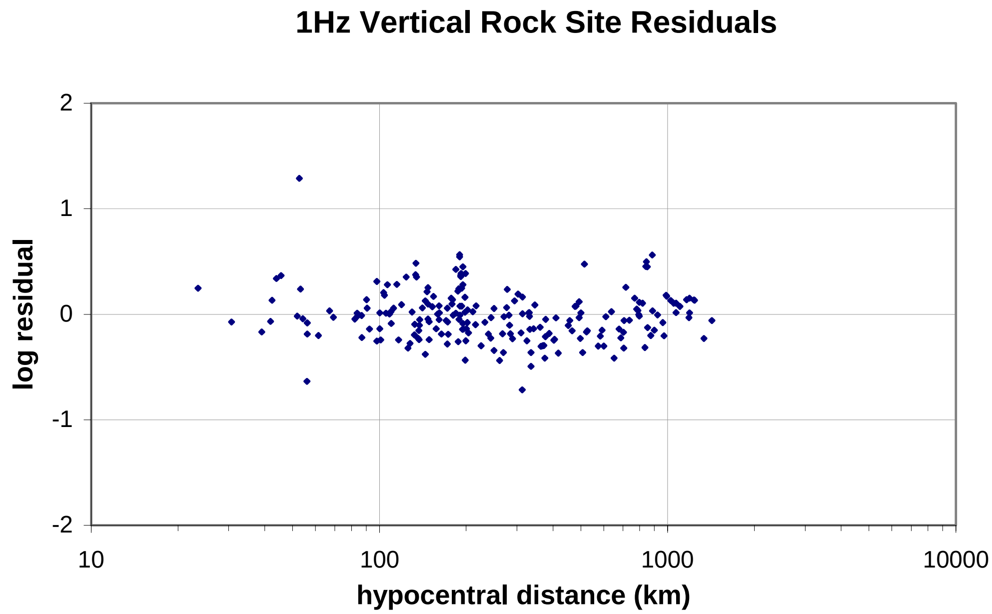

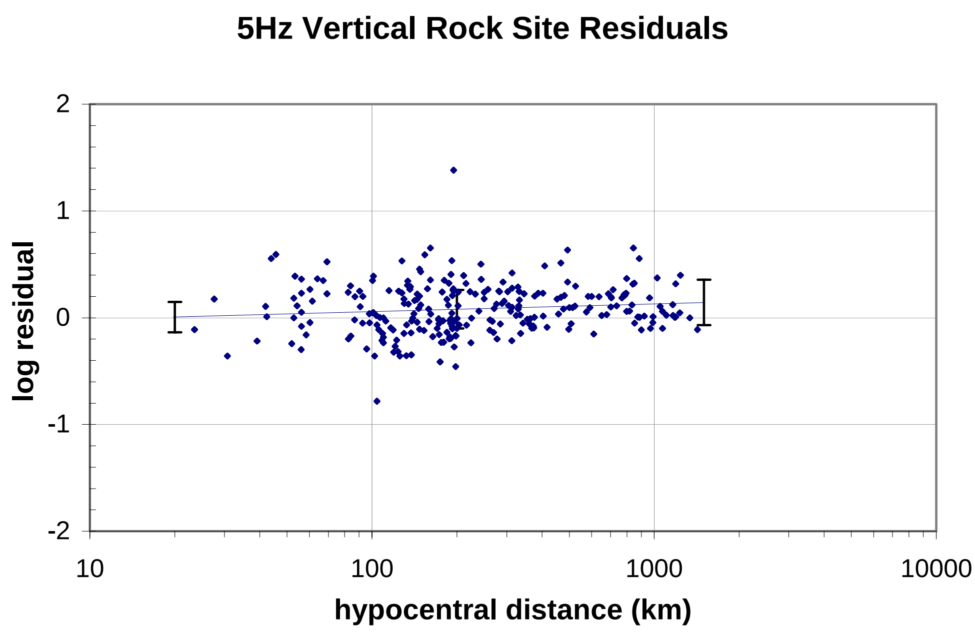

Figure 4.1: Vertical component Fourier acceleration residuals from rock sites, plotted at 1Hz and 5Hz. Line in (b) is least-squares regression of data, and error bars show standard error of the regression coefficients. log(resid) = log(obs) – $GMA04_Z$

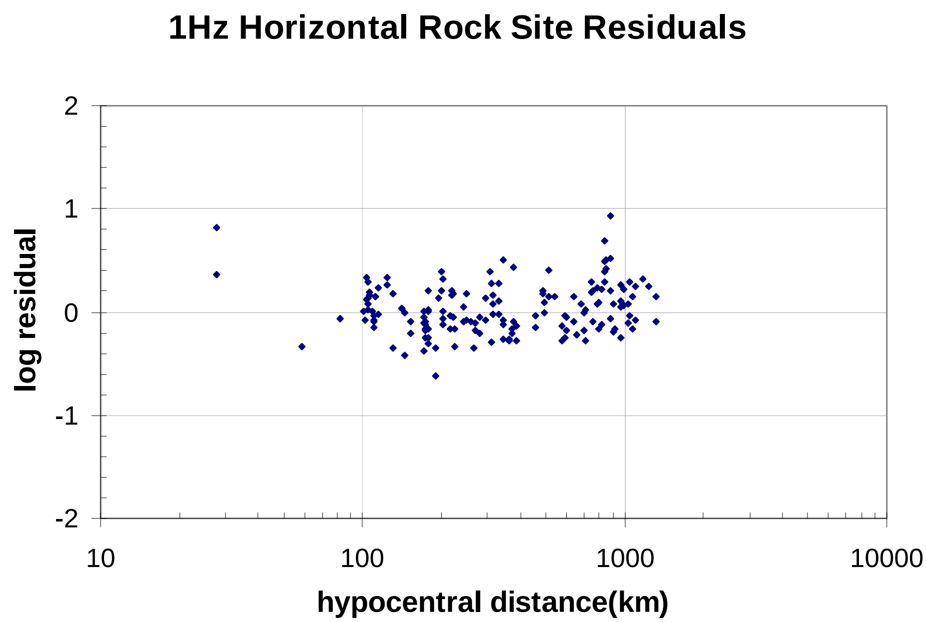

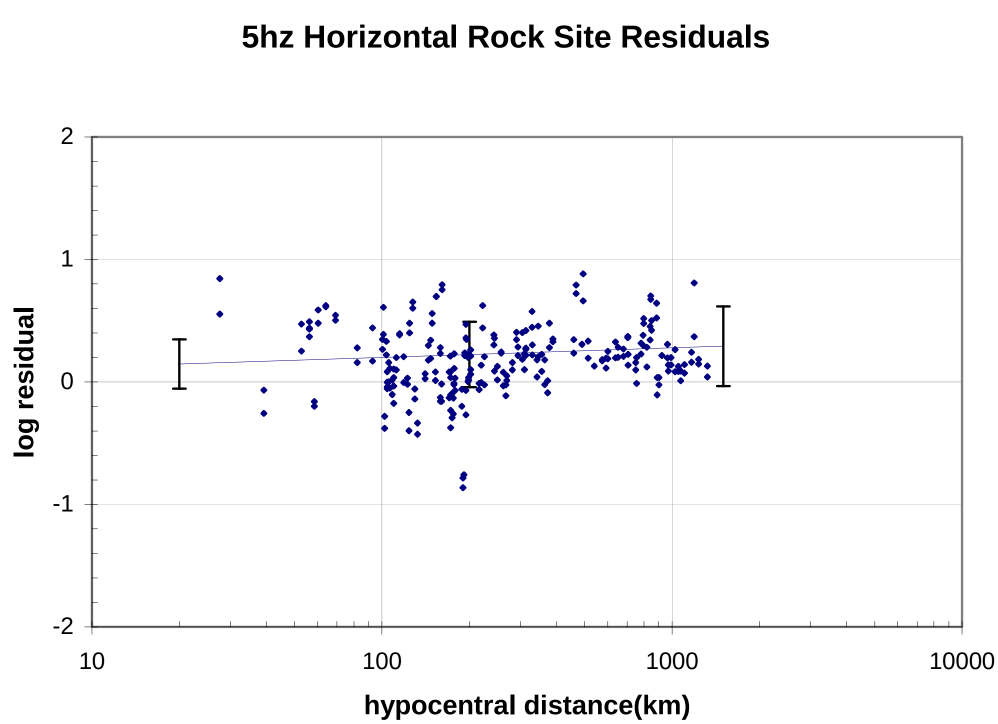

Figure 4.2: Horizontal residuals from rock sites, plotted at 1Hz and 5Hz. Line in (b) is least-squares regression of data, and error bars show standard error of the regression coefficients. log(resid) = log(obs) – $GMA04_H$

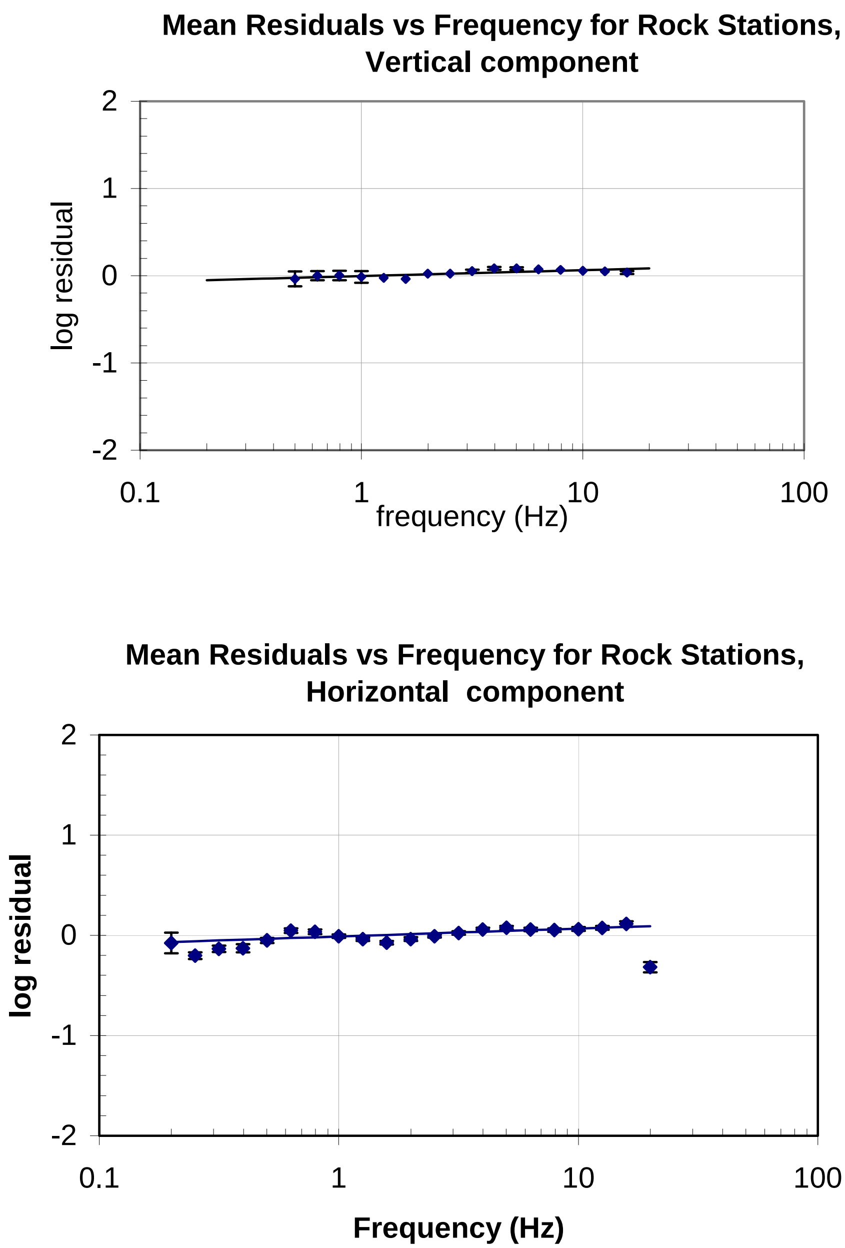

Figure 4.3: Mean residuals from rock stations, averaged per frequency bin and plotted from 0.2 to 20Hz for vertical (a) and horizontal (b) components. Error bars show standard error of the mean. (a) log(resid) = log(obs) – $GMA04_Z$ (b) log(resid) = log(obs) – $GMA04_H$

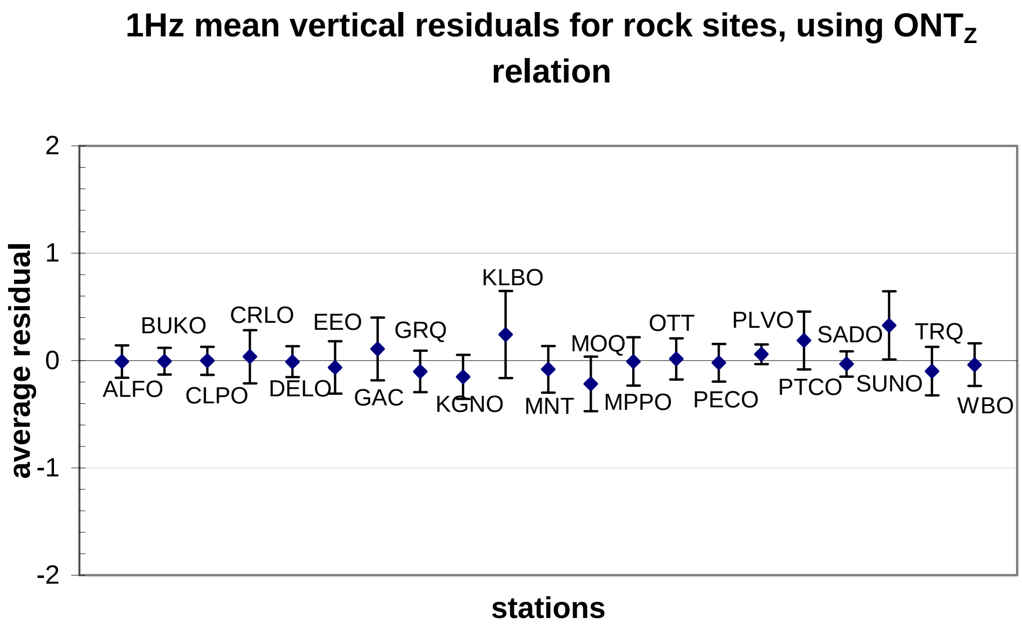

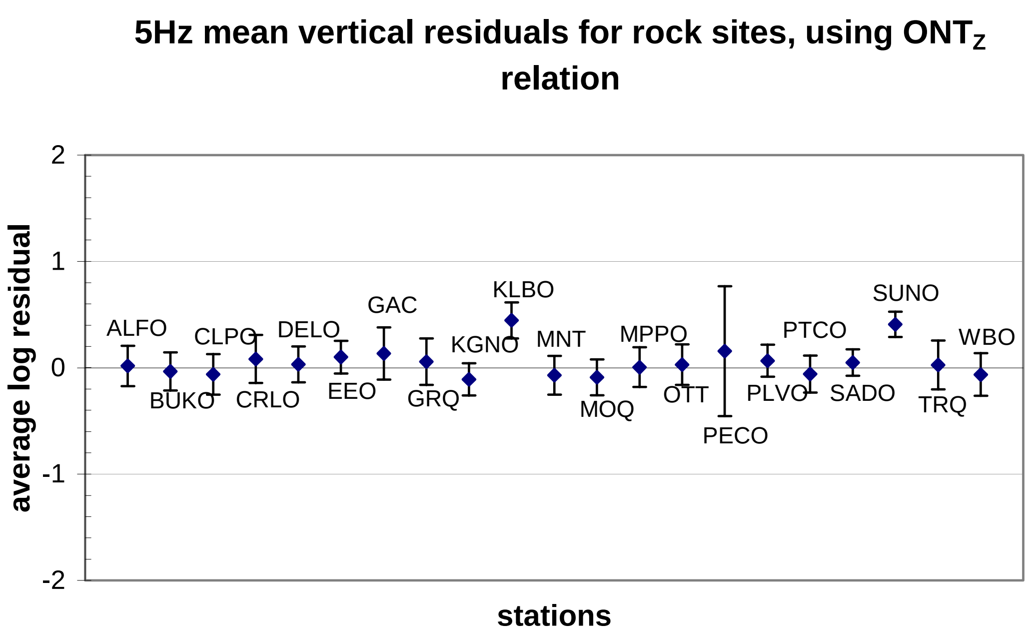

Figure 4.4: Mean vertical residuals, averaged per station, plotted at 1Hz and 5Hz. Error bars represent one standard deviation. log(resid) = log(obs) - ONT_Z

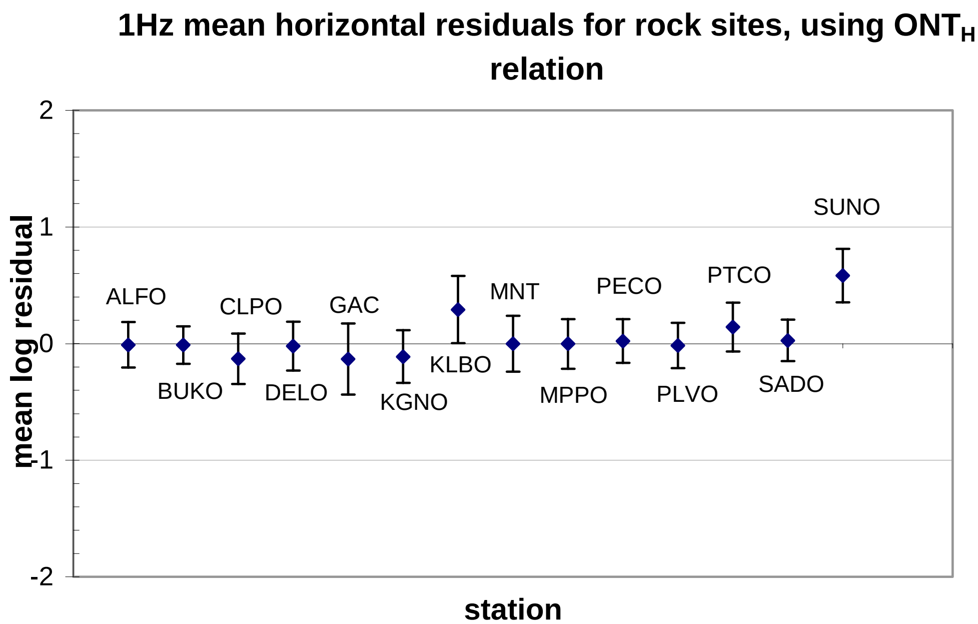

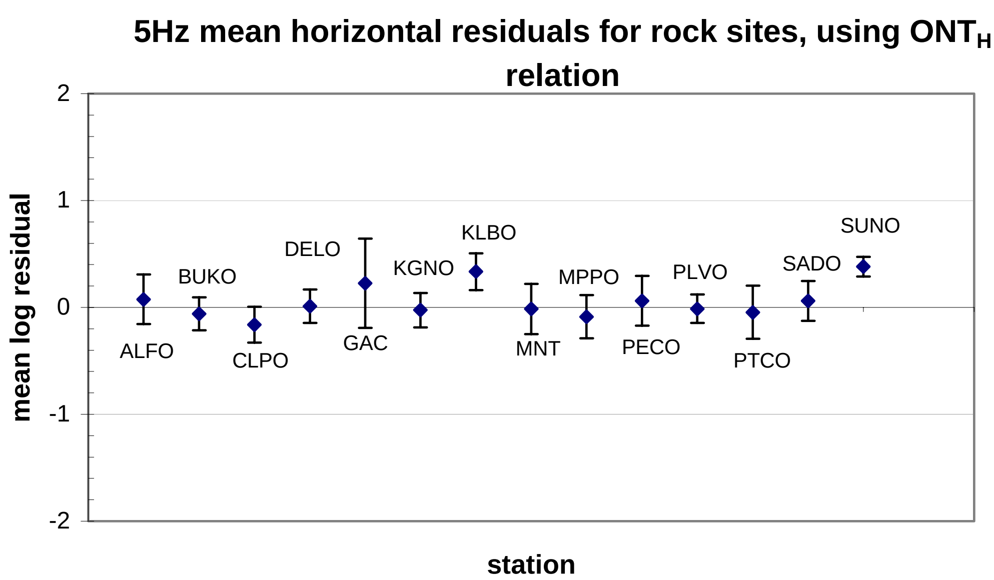

Figure 4.5: Mean horizontal residuals, averaged per station, plotted at 1Hz and 5Hz. Error bars represent one standard deviation. log(resid) = log(obs) – ONT_H

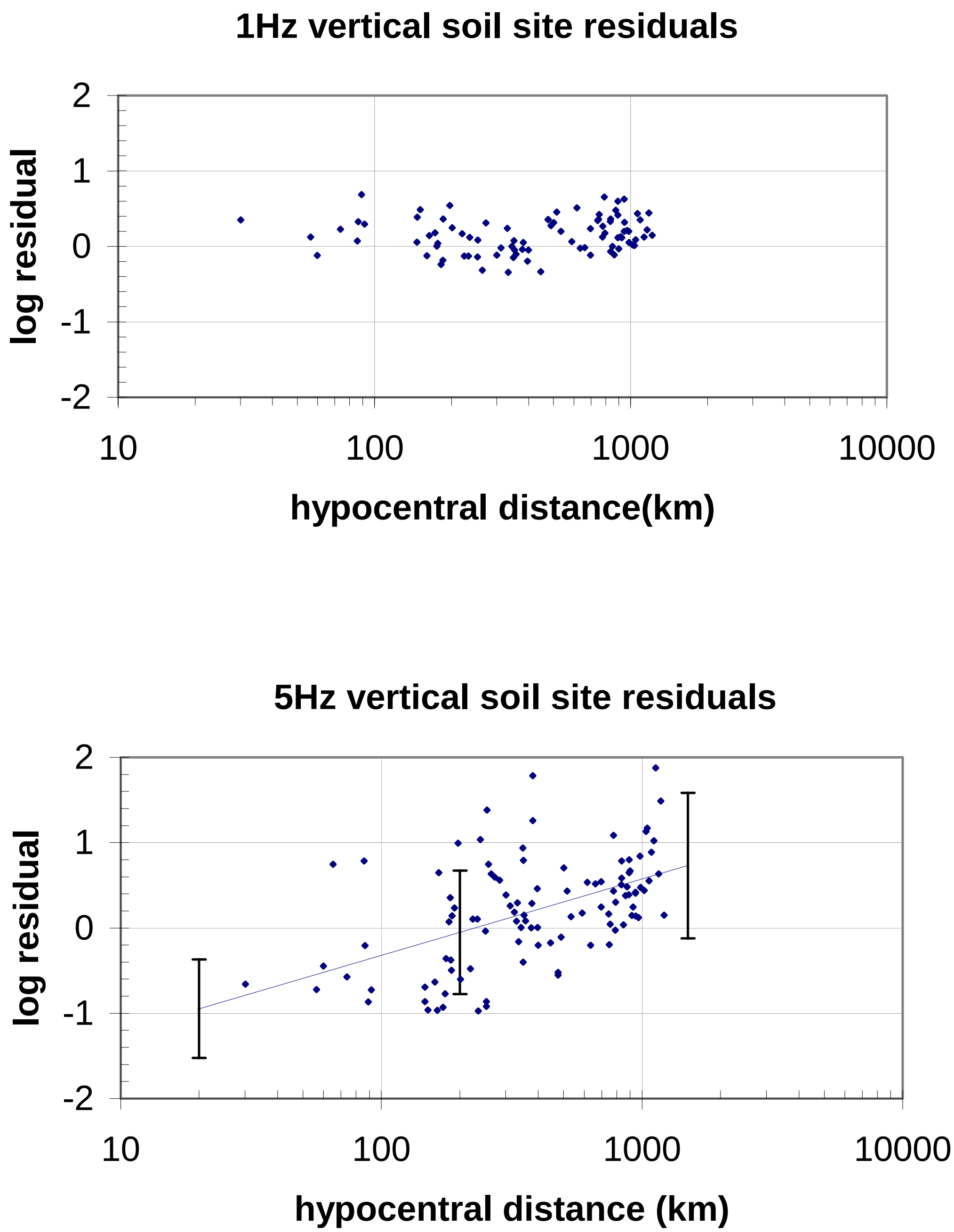

Figure 4.6: Vertical residuals from soil sites, plotted at 1Hz and 5Hz. Line in (b) is least-squares regression of data, and error bars show standard error of the regression coefficients. log(resid) = log(obs) – ONT_Z

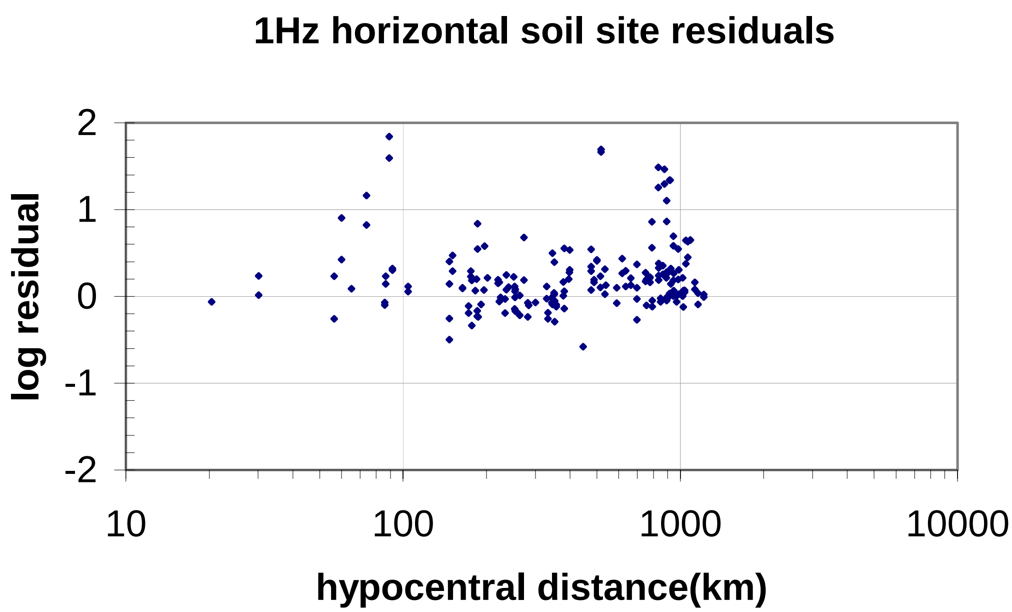

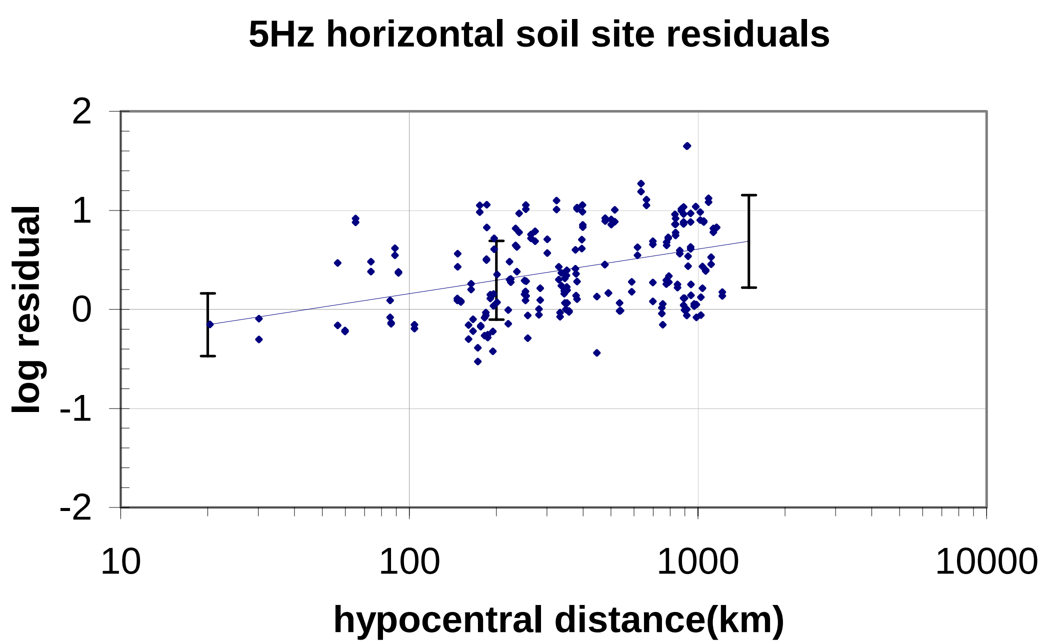

Figure 4.7: Horizontal residuals from soil sites, plotted at 1Hz and 5Hz. Line in (b) is least-squares regression of data, and error bars show standard error of the regression coefficients. log(resid) = log(obs) – ONT_H

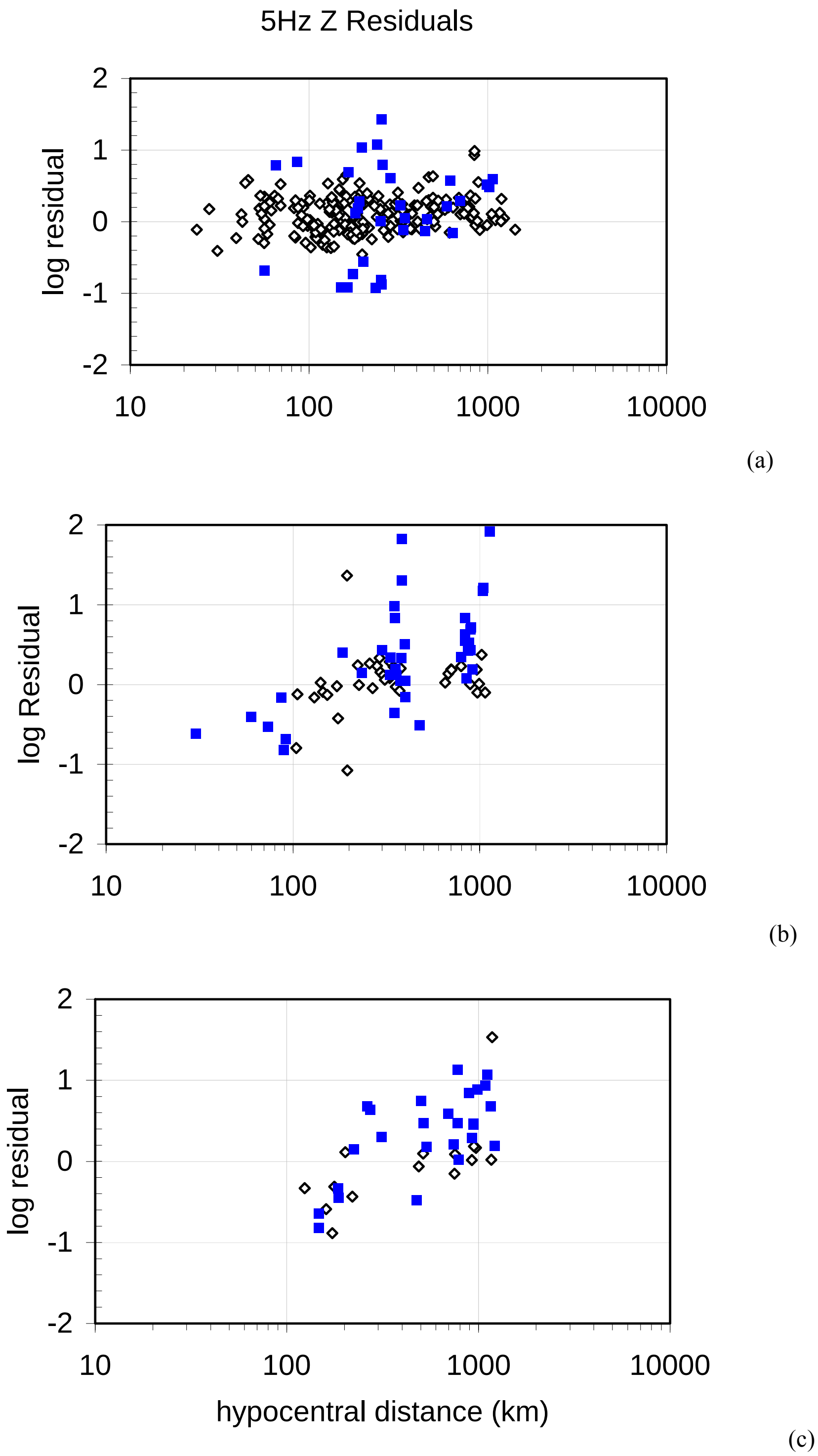

Figure 4.8a,bc: Vertical component residuals at 5Hz. Diamonds represent bedrock stations, squares are soil stations. (a) Eastern Ontario and Western Quebec, (b) Central Ontario, (c) Southwestern Ontario log(resid)=log(obs) – GMA04$_Z$

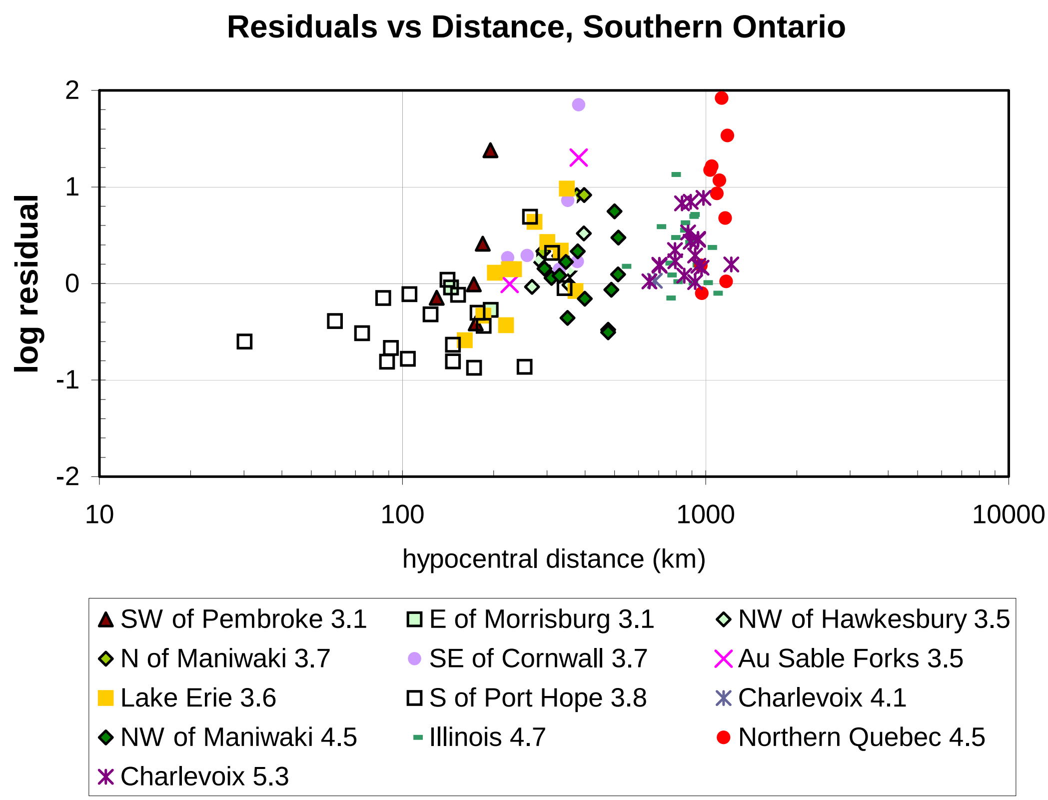

Figure 4.9: Vertical component residuals at 5Hz, all stations in southern Ontario (southwestern and central Ontario combined). Shapes refer to source regions: Diamonds: Western Quebec (WQSZ). Squares: Ontario. Stars: Charlevoix. X : Au Sable Forks, NY. Other events as indicated. log(resid) = log(obs) – $GMA04_Z$

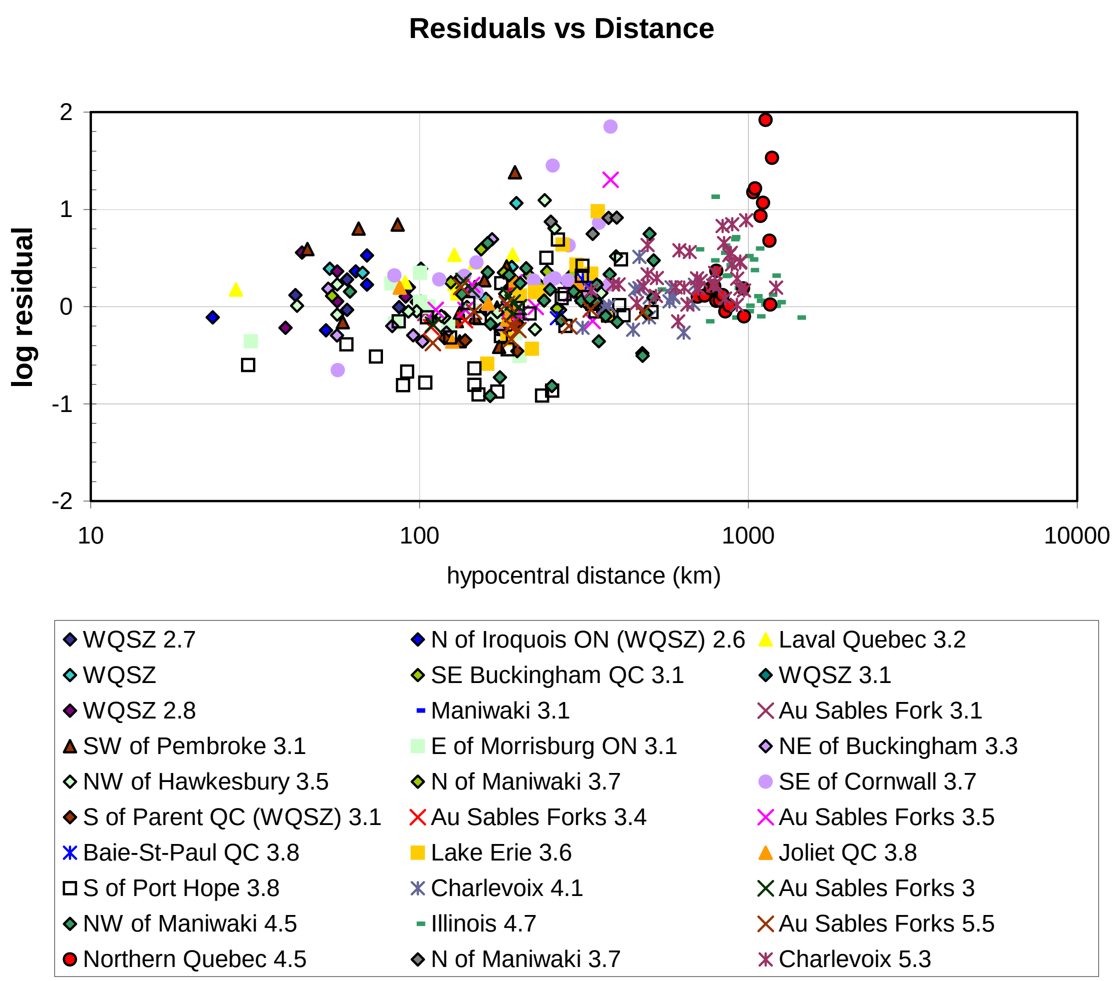

Figure 4.9: Vertical component residuals at 5Hz, recorded at all stations in the study region. Shapes refer to source regions: Diamonds: Western Quebec (WQSZ). Squares: Ontario. Stars: Charlevoix. X : Au Sable Forks, NY. Other events as indicated. log(resid) = log(obs) – $GMA04_Z$

4.2: Horizontal to Vertical Spectral Ratio Results

4.2.1 Rock Station HVSRs:

The following amplification spectra are plotted on a logarithmic scale to stay consistent with the calculations and previous literature. However, for clarity, the results are discussed in terms of their non-logarithmic values.

Figure 4.11 shows the H/V spectra for rock stations within the study area. All spectra plot close to zero, with the exception of GAC, which plots well below zero at low frequencies. This anomaly could be related to an instrument response problem. The mean H/V trend from Figure 4.12 is 0.94 ±1.3 at 1Hz, and 1.2 ±1.1 at 5Hz. The mean H/V is within one standard deviation of zero from 0.25 to 2Hz. Thus, it appears that at higher frequencies, there is some amplification of the horizontal component at all of the rock stations. This agrees with previous studies: Boore and Joyner (1997) found amplifications of less than 1.2 at very hard rock sites, while Siddiqi and Atkinson (2002) found an average amplification of 1.09 ±0.24 at 1Hz and 1.48 ±0.51 at 5Hz in eastern Canada.

Individual stations show wide variability below 1Hz, this is interpreted to be due to a sparse dataset below this level.

Station KLBO has a peak of 1.4 at 1.3Hz. The comparatively high amplitude at this site may possibly be due to topographic effects as it is located at top of a 30m hill.

ALFO shows a strong peak at 3.2 Hz with an H/V of 1.8. Average amplification at this site is also fairly high at 1.3. Surficial geology of the region surrounding the site may play a role in higher than expected amplification here. Siddiqi and Atkinson (2002) observed a correlation between amplification of higher frequencies at rock sites and the surficial geology of the surrounding region. The site is located in an area classified as a clay plain by Chapman and Putnam (1985). Clay is known to significantly amplify ground motions due to its low shear wave velocity.

All rock sites are located on crystalline bedrock, with the exception of PECO and PTCO, which are located on Paleozoic bedrock. Although these sites show relatively high amplification at 15 Hz, with peaks of 1.5 and 1.7, neither show any defined peak or amplification significantly higher than the average hard rock site (average amplification at 1Hz and 5Hz of the Paleozoic sites are 1.0 ±1.1 and 1.4 ±1.0). For this reason, these sites were included as part of the rock reference database for the attenuation study.

4.2.2: Soil Station HVSRs

A major objective of this study was to characterize the site response at each soil station in Ontario. To do this, the common HVSR approach is displayed and discussed here. In Section 4.2.3, the regional ground motion method is compared to the HVSR, discussing any noteworthy differences between the two methods.

The H/V ratio varied significantly between soil stations, as expected from the geology. The mean for the study area is shown in Figure 4.13. The mean amplification recorded by soil stations is 1.3 ±1.9 at 1Hz and 1.9 ±1.7 at 5Hz.

The H/V spectra are plotted for each station in Figures 4.14, 4.15 and 4.16, in the order they are discussed. Table 4.2 summarizes the fundamental frequency, peak amplification, and average amplification (between 0.5Hz and 16Hz) for every soil station.

The stations can be grouped into three categories, based on the shape of their spectra:

Stations with flat spectra (Figure 4.14): Several stations show very little amplification across the entire spectrum. These stations are: ELGO, HGVO, and PLIO.

ELGO and HGVO are both Paleozoic limestone stations, but the surface layers were observed to be highly weathered and friable (Murphy, 2003). Because of this, they were not included in the rock database. They show low average amplification values of 1.2 ±1.3 and have peak amplitudes at 2.0, which are higher than any of the rock sites included in this study, but agree with previous studies of amplifications at rock stations, such as Boore and Joyner (1997). PLIO (Pelee Island) shows the flattest spectrum of all the non-hardrock sites, with an average amplification of 1.1. A small peak of amplitude 1.7 is observed at 2.5Hz. The station location plots in a "beveled till plain" region on the Physiography Map of southern Ontario (Chapman and Putnam, 1984), although it is located very near to an area of "limestone plain". It is interpreted then, from the surficial geology information and the HVSR results, that there is likely only a very thin overburden layer at this site.

Stations showing a well-defined spectral peak (Figure 4.15): Stations ALGO, BANO, BRCO, KSVO, STCO, and TYNO show well developed peaks that may represent the fundamental mode frequencies. These peaks occur as indicated in Table 4.2.

STCO shows a broad peak at 5Hz. Based on shear-wave refraction data from Beresnev and Atkinson (1997). STCO is characterized by a 20m thick low velocity (300m/s) layer above the Paleozoic bedrock (1800m/s). By Equation 1.3, this would correspond to a fundamental frequency of 3.8Hz. This is in fair agreement with the HVSR peak at 5Hz. In a separate shear-wave refraction survey, Murphy (2002) found a layer depth of 17m and a shear wave velocity of 320m/s which would give a theoretical fundamental frequency of 4.7Hz. This is in good agreement with our data.

A similar response is observed at TYNO, with a broad peak of 17 at 4Hz. Beresnev and Atkinson (1997) estimated a three-layer velocity profile containing a nine metre thick low velocity (240m/s) layer on top of a twenty-two metre layer of 570m/s which in turn is on top of bedrock with a velocity of 3380m/s. The soil layers would theoretically produce a fundamental peak at 4.2Hz, although the multiple layers would complicate the spectrum. This is in excellent agreement with the HVSR estimate.

The BRCO HVSR function shows a very high peak of 16 at 2Hz. The refraction study of Bersenev and Atkinson (1997) showed a 20m thick 240m/s layer overlaying a 34m thick 430m/s layer on top of bedrock at 1160m/s. The survey revealed the subsurface topography is not flat however, with soil deposits dipping to the east. This gave a fundamental frequency peak at 4Hz, which is in excellent correlation with the peak frequency observed in the H/V spectrum.

The other three sites are located in areas of rough topography with unknown soil thickness. In particular, ALGO is located on a glacial sand deposit, at the summit of a 30m topographic high. This site has a simple H/V spectrum, with a well-defined peak amplitude of 6.6 at 4Hz, which is a reasonable fundamental frequency considering Equation 1.3.

Stations with complex spectra (Figure 4.16): ACTO, CLWO, LINO, MEDO, PEMO, PKRO, TOBO, TORO, and WLVO have complex functions where no single peak was well defined. PEMO, CLWO, and TOBO have rough surface topography and/or subsurface bedrock topography. TOBO, PEMO, WLVO and LINO show progressively increasing amplification with frequency, which could be due to a fundamental frequency beyond 20Hz.

TORO is located on a spit of man-made landfill and sand deposits in the Toronto harbour. These deep, loose sediments could account for the low fundamental frequency (1Hz) and the high amplification (9.3) observed at this site. A clear peak of 3.8 is also observed at 5Hz. A better understanding of the geology at this site is needed to explain this, although it could be related to the presence of two subsurface layers.

Correlation between spectral amplification and soil thickness

Based on the shear-wave velocity profiles of Beresnev and Atkinson (1997) and Murphy (2003) as well as field observations, the sites were seperated into categories representing soil depth. ALGO, BRCO, PKRO, TORO, and TYNO have a thick soil layer (>20m), ACTO, STCO, and WLVO have a moderate soil depth (between five and twenty metres), and stations ELGO, HGVO, PLIO and LINO have a very shallow (<5m) soil layer. The averages for the three categories are shown in Table 4.3, with deep soil sites showing a low fundamental frequency and high amplification, and shallow sites having no clear fundamental frequency between 0.5 and 16Hz. Thus, the results show good correlation with soil depth. By comparison to these averages, the approximate soil depth can be inferred at other stations, with the caution that other factors such as topography may influence the observed spectra.

4.3 Ground Motion Residual Spectra Results and Discussion

Since it was shown that bedrock sites experience little site amplification, and since the ground motion observed at Ontario rock stations was modeled in section 4.1, then the observed ground motion spectrum at a soil site can be divided by the modeled ground motion to give an estimate of site amplification. In this section, the residual method is compared to the HVSR method.

Residual Spectra are also plotted in Figures 4.14, 4.15 and 4.16 for the horizontal components of stations located on overburden, as well as two stations located on weathered Paleozoic bedrock (HGVO and ELGO). The peak amplitudes and fundamental frequencies and average spectral amplification are summarized in Table 4.2.

For all plots, log(residual) = log(observed) – ONT_H. Since there was no definitive conclusion for the origin of the observed residual – distance trend, there are no corrections made to account for this. Because the goal of this section is to characterize site response at individual stations, and since most stations measure ground motion from a wide range of hypocentral distances, specific path effects may average out over the database.

The residual spectra from the regression analysis plotted, for the most part, very close to the HVSR. Above 0.4Hz, the residual method gives an estimate of average amplification slightly higher than that of the HVSR, although well within one standard deviation. It is possible that there is some soil amplification of the vertical component which would cause the HVSR method to underestimate the amplification. This difference is observed in Figure 4.17, which shows the HVSR and Residual spectra for all non-rock stations.

For stations that showed flat H/V spectra (ELGO, HGVO, PLIO), the residual method showed excellent correlation. The average percent difference between the three stations for both the peak amplitude and average amplitude is about 10%.

The residual spectra also resolves the peaks observed in the HVSR spectra for ALGO, BANO, KSVO, STCO, and TYNO, and BRCO, to within one frequency bin. However, for stations ALGO and BANO, the residual amplitude remains amplified after the main peak. This phenomenon was also observed at these stations by Murphy (2003) in a study of Standard Spectral Ratios. The reason for this remains unclear, but it could be due to unreliable instrument response at frequencies higher than 8-10Hz. (D. Motazedian, pers. com.) Another possibility is a complex site response exists due to rough topography that is unresolved by the HVSR method.

At stations TYNO and BRCO, secondary peaks are observed at 10Hz and 5Hz respectively, which could again be due to a complex site response. This suggestion agrees with Beresnev and Atkinson (1997) where the shear-wave velocity at these sites was modeled as a three-layer profile, which produced theoretical spectra with secondary peaks at approximately 9Hz and 4Hz for TYNO and BRCO respectively. The HVSR method did not resolve these.

The residual and H/V methods correspond reasonably well at stations that show complex spectra. Below 1Hz, however, there is only a fair correlation, with many stations showing sharp peaks in the residual spectra. Due to more stringent magnitude-distance requirements below 1Hz, the database of low frequency ground motions is much sparser, particularly for the regional regression study. A comparison of the two techniques is shown in Table 4.2.

In addition, the results of the HVSR study and the numerical modeling results of Murphy and Eaton (2004), and Murphy (2003) are shown in Table 4.2. The fundamental frequency peak, peak amplification, and average amplification between the methods are shown. The average spectral amplification is not shown for the other studies since they calculate their averages over a different range of frequencies.

The peak frequencies of the HVSR and the regional ground motion comparison differ by 28%. The peak amplitudes show a 54% difference, and the average amplifications differ by 43%.

This HVSR study differs from that of Murphy and Eaton by 21%, and 49% for the fundamental frequency and peak amplitude values. The ground motion residual study estimates for the fundamental frequency and peak amplitude differ from Murphy and Eaton's HVSR values by 24%, and 42% respectively. Finally, when compared to theoretical studies based on shear wave refraction data, the regional ground motion results differ by 40% for the fundamental frequency, and 47% for the peak amplitude on average. In general the peak frequency was resolved well in comparison to theoretical results and other studies. The residual method tended to have slightly higher peak values than the other studies, while the HVSR method resulted in peak amplification lower than any of the other studies.

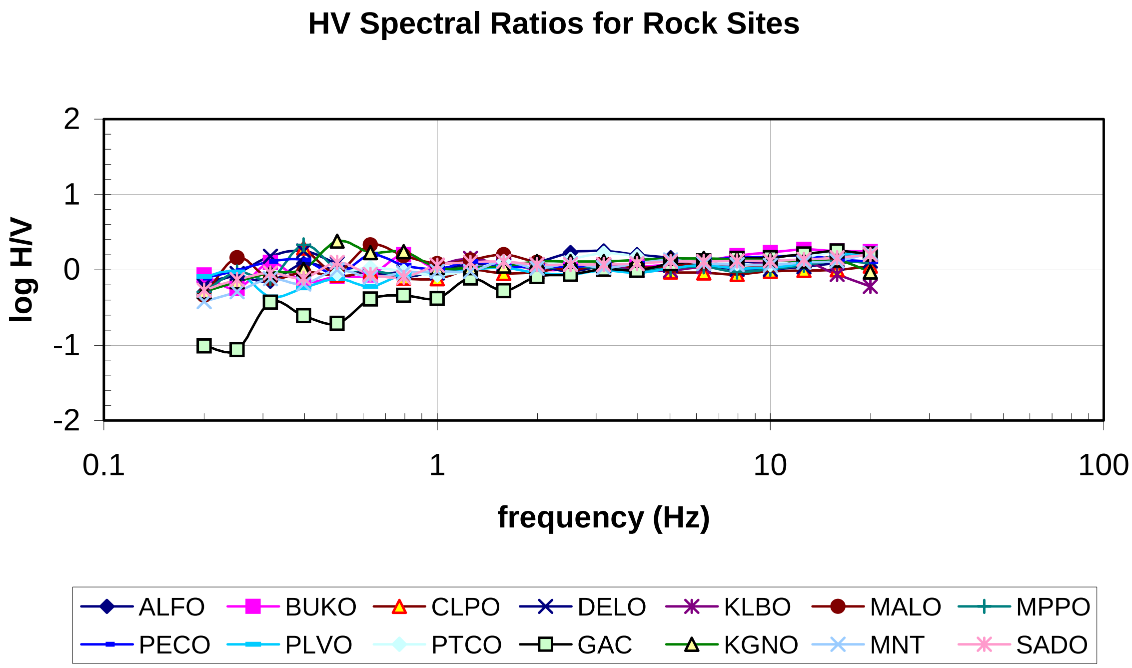

Figure 4.11: H/V Spectral ratios for rock stations, plotted from 0.2 to 20Hz.

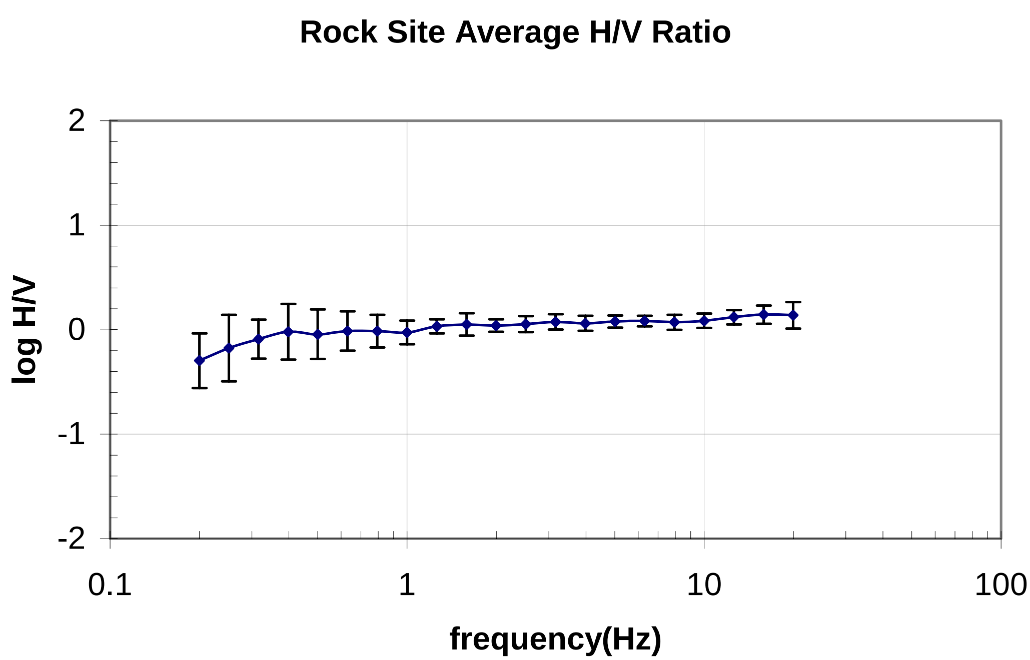

Figure 4.12: Mean H/V ratio, averaged per frequency bin and plotted from 0.2 to 20Hz. Error bars show one standard deviation.

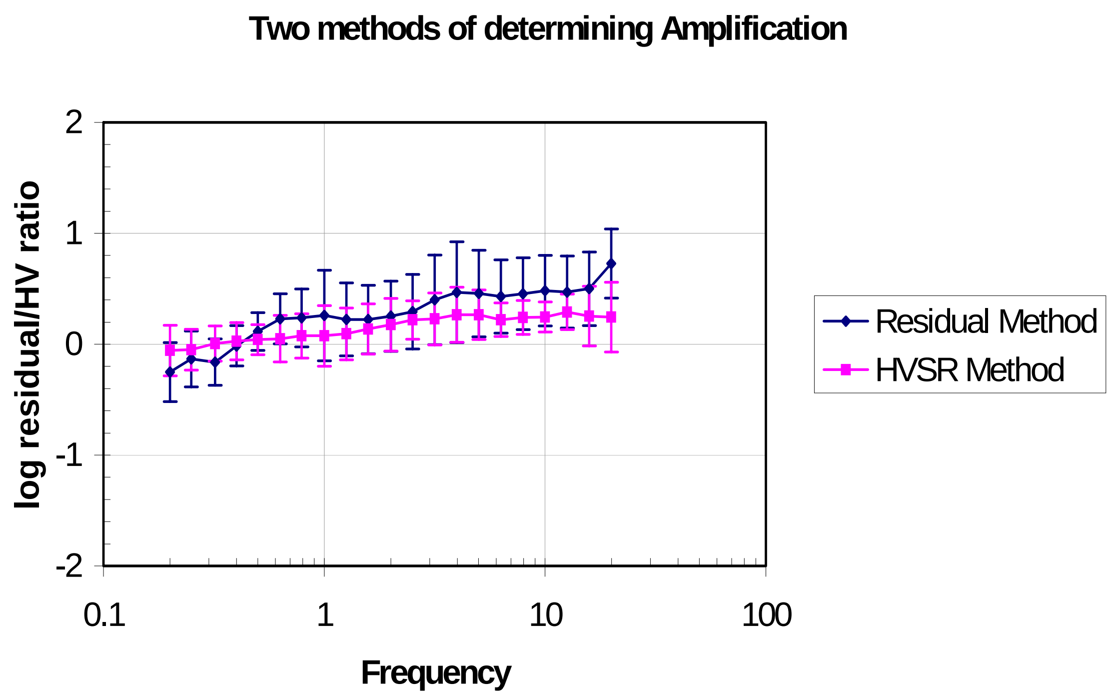

Figure 4.13: Mean H/V ratio and regression residual spectrum for soil sites, averaged per frequency bin from 0.2 to 20Hz. Error bars represent one standard deviation. log(res) = log(obs) - ONT_H

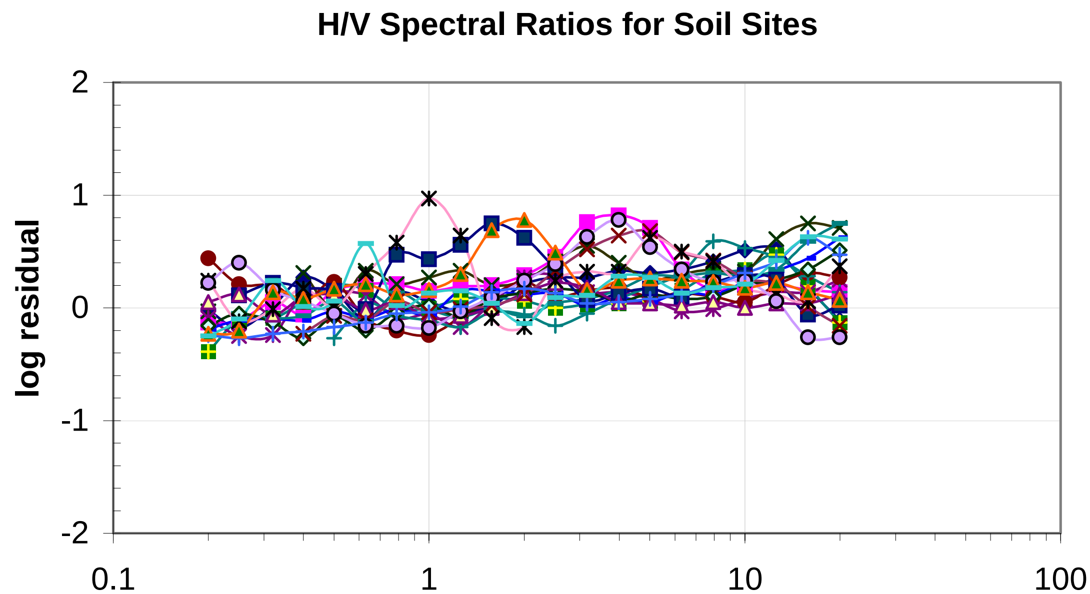

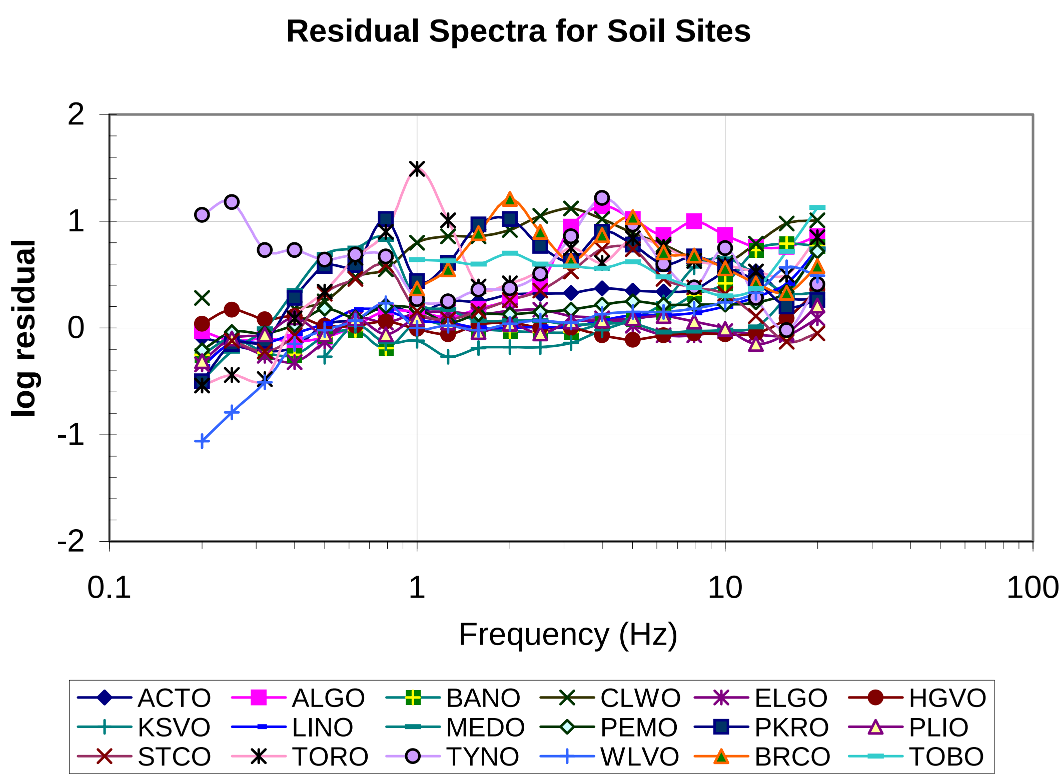

Figure 4.17: HVSR (a) and Horizontal residual spectra from regional ground motion study (b), for soil sites. Plotted from 0.2 to 20Hz. log(resid) = log(obs) - ONT_H

Study:	Regression Residuals			HVSR			Murphy and Eaton HVSR		Theoretical*	
Station	f_0 (Hz)	Peak A	Avg A	f_0 (Hz)	Peak A	Avg A	f_0 (Hz)	Peak A	f_0 (Hz)	Peak A
ACTO	12.6	3.4	2.0	12.6	3.3	1.7	12.6	5.0	10.0	4.7
ALGO	4.0	13.8	3.4	4.0	6.6	2.1	4.0	11.0		
BANO	15.9	6.2	1.4	12.6	3.0	1.4	12.5	4.6		
BR CO	2.0	16.2	5.1	2.0	6.0	1.9	2.0	10.4	1.8	9.5
CLWO	3.2	13.2	6.1	15.9	5.6	2.2				
ELGO	2.5	1.5	1.1	2.5	1.9	1.2	25.1	3.2	11.3	2.3
HGVO	20.0	2.3	1.0	15.9	2.0	1.2	15.8	3.7		
LINO	20.0	5.5	1.3	20.0	4.2	1.3	15.8	3.7	12.3	9.5
KSVO	10.0	4.6	1.1	7.9	3.9	1.2	9.7	10.7		
MEDO	0.8	6.8	1.6	20.0	5.6	1.4				
PEMO	20.0	5.2	1.5	20.0	3.2	1.2	22.4	6.9		
PKRO	2.0	10.5	4.7	1.6	5.6	1.9	1.8	9.2	1.8	9.5
PLIO		1.6	1.0		1.7	1.1				
STCO	4.5	5.5	2.2	5.0	4.8	1.7	4.5	7.0	3.4	9.5
TOBO	20.0	13.5	3.6	15.9	4.3	1.6				
TORO	1.0	30.9	4.8	1.0	9.3	2.1				
TYNO	4.0	16.6	3.5	4.0	6.0	1.5	4.0	11.5	4.2	10.6
WLVO	15.9	3.7	1.4	15.9	4.2	1.3	12.6	4.9	12.0	5.7

Table 4.2: Comparison of two techniques from this study as well as results from other studies. *Theoretical values for ACTO, BRCO, PKRO, STCO, TYNO and WLVO from Murphy and Eaton (2004), based on refraction results from Beresnev and Atkinson (1997). Theoretical results for ELGO and LINO from Murphy (2003).

Approximate soil thickness	Regression Residual Study			HVSR Study		
	f0 (Hz)	Peak A	Average A	f0 (Hz)	Peak A	Average A
Deep (>20m)	2.6±1.2	17±7	4.3±0.7	2.5±1.2	6.7±1.3	1.9±0.2
Moderate (5-20m)	11±5	4.2±0.9	1.8±0.4	11.2±4.5	4.1±0.6	1.5±0.2
Very Shallow (<5m)	-	2.7±1.9	1.1±0.1	-	2.5±1.2	1.2±0.1

Table 4.3: Average fundamental frequency, peak amplification, and average amplification for sites with known soil depths.

5.0 Conclusions

The main objectives of this study were:

1. to determine if ground motion in the study area follows the regional trend, and if not, to create a modified model for southern Ontario and western Québec;
2. to characterize site response spectra for POLARIS stations using horizontal-to-vertical ratios and a spectral comparison between observed ground motion and that predicted by the regional hard-rock relations; and
3. to compare the two methods of site response estimation.

With regards to the first objective, ground motions from a database of twenty-nine small-to-moderate events were compare reasonably well to those predicted by the Atkinson (2004) ground motion model for eastern North America. However, amplitudes in Ontario are slightly amplified at high frequencies compared to the eastern North American model.

In south-central and southwestern Ontario, observed ground motions are lower than predicted at small hypocentral distances, and higher than predicted at large distances, although this trend may actually be a superposition of amplitudes from several well-recorded events. It is possible that crustal structures are providing a good waveguide for travel oriented northeast–southwest, although further study and a larger database from events with various azimuths would be necessary to reach a definitive conclusion on this observation.

Site response at POLARIS stations was characterized by plotting estimates of spectral amplification using two methods (HVSR and regional ground motion residuals).

There was very little near-surface amplification observed at rock stations. As expected, sites located on shallow overburden show relatively flat amplification spectra, devoid of any obvious peaks, while sites located on deep soils have in general a strong peak at a frequency represented by the fundamental resonance mode.

The third objective of this thesis was to compare the regional ground motion comparison method (where the observed amplitude spectrum is divided by the spectrum predicted by the regional ground motion model) to the frequently used, but somewhat controversial Horizontal-to-Vertical spectral ratio approach. The results from the two techniques are in good comparison, particularly the estimated fundamental frequencies. Overall, the HVSR have lower amplification estimates than the regional ground motion residual spectra. This may be due to some amplification of vertical component, thus negatively effecting the H/V calculation, or possibly due to regional waveguide effects contaminating the site response estimate. It appears that while both methods are able to resolve the fundamental frequency peak due to a simple soil layer, the ground motion residual method may be more sensitive in resolving complexities in the amplification functions caused by dipping bedrock interfaces or multiple layers.

The two methods also compare well with other studies, with the regional ground motion technique showing the best correlation with various theoretical and empirical studies by Beresnev and Atkinson (1997) and Murphy and Eaton (2005).

6.0 References

Adams, J., Basahm, P.W.: "The seismicity and seismotectonics of Canada east of the Cordillera." Geoscience Canada Vol 16, pg 3-16. 1989.

Al Yuncha, Z., and Luzón, F.: "On the horizontal-to-vertical ratio in sedimentary basins." Bulletin of the Seismological Society of America, Vol. 90, pg 1101-1106. 2000.

Atkinson, G.M.: "Empirical attenuation of ground-motion spectral amplitudes in southeastern Canada and the northeastern United States.", Bulletin of the Seismological Society of America, Vol. 94, pg 1079-1095. 2004.

Atkinson, G.M.: Errata for: "Empirical attenuation of ground-motion spectral amplitudes in southeastern Canada and the northeastern United States." Bulletin of the Seismological Society of America. *in press*.

Atkinson, G.M. and Cassidy, J.F. "Integrated use of seismograph and strong-motion data to determine amplification: response of the Fraser River delta to the Duvall and Georgia Strait earthquakes." Bulletin of the Seismological Society of America, Vol. 90, pg 1028 – 1040. 2000.

Atkinson, G.M. and Mereu, R.: "The shape of ground motion attenuation curves in southeastern Canada." Bulletin of the Seismological Society of America. Vol. 82, 2014-2031. 1992.

Bard, P.: "Effects of surface geology on ground motion: Recent results and remaining issues," in Duma, G (editor) "Proceedings of 10th European Conference on Earthquake Engineering." Vol 1. 1995.

Boyce, J.I., and Morris, W.A.: "Basement-controlled faulting of Paleozoic strata in southern Ontario, Canada: new evidence from geophysical lineament mapping." Tectonophysics, Vol. 353, pg 151-171. 2002.

Beresnev, I.G., and Wen, K.L: "The accuracy of soil response estimates using soil-to-rock spectral ratios." Bulletin of the Seismological Society of America, Vol. 86, pg 519-523, 1996.

Boore, D. M., SMSIM; Fortran programs for simulating ground motions from earthquakes; version 1.0, U.S. Geol. Surv. Open-File Rept. 96-80-A , 1996.

Boore, D.M., and Joyner, W.B. "Site amplifications for generic rock sites." Bulletin of the Seismological Society of America, Vol. 87, pg 327-341. 1997.

Chapman, L.J., and Putnam, D.F.: "Physiography of Southern Ontario." Ontario Geological Survey Map P.2715 (coloured). Scale: 1:600 000. 1984.

Cooley, T.W., and Tukey, J.W.: "An algorithm for the machine calculation of complex Fourier series." Mathematical Computation, Vol. 19, pg 297-301. 1965.

Field, E.H., and Jacob, K.H.: "A comparison and test of various site-response estimation techniques including three that are not reference-site dependent". Bulletin of the Seismological Society of America, Vol. 85, pg 1127-1143. 1995.

Joyner, W.B., Warrick, R.E., and Fumal, T.E.: "The effect of Quaternary alluvium on strong ground motion in the Coyote Lake, California, earthquake of 1979." Bulletin of the Seismological Society of America, Vol. 71, 1333-1349, 1981.

Kaka S., and Atkinson, G.M,: "Relationships between instrumental ground-motion parameters and modified Mercalli intensity in eastern North America." Bulletin of the Seismological Society of America, Vol. 94, 1728-1736. 2004.

Lermo J., and Chávez-García, F.J.: "Site effect evaluation using spectral ratios with only one station." Bulletin of the Seismological Society of America, Vol 83, pg 1574-1594. 1993.

Molnar, S. Cassidy, J.F., Dosso, S.E. "Site response in Victoria, British Columbia from spectral ratios and 1D modelling." Bulletin of the Seismological Society of America, Vol. 94, pg 1109-1124. 2004.

Murphy, C: "Near surface characterization and estimated site response at POLARIS seismograph stations in Southern Ontario, Canada." Master of Science Thesis. Department of Earth Sciences, University of Western Ontario. 2003.

Murphy C., and Eaton, D: "Empirical Site Response for POLARIS Stations in Southern Ontario, Canada", Seismological Research Letters, *in press.*

Nakamura, Y.: "A method for dynamic characteristics estimation of the subsurface using microtremors on the ground surface," Quarterly Report of the Railway Technical Research Institute, Vol 30, pg 25-33. 1989.

Siddiqqi, J. and Atkinson, G.M.: "Ground-motion amplification at rock sites across Canada as determined from the horizontal-to-vertical component ratio." Bulletin of the Seismological Society of America, Vol. 92, pg 877-884. 2002.

White, D.J., Forsyth, D.A., Asudeh, I., Carr, S.D., Wu, H., Easton, R.M., Mereu, R.F., "A seismic-based cross-section of the Grenville Orogen in southern Ontario and western Québec." Canadian Journal of Earth Sciences, Vol. 37, pg 183-192. 2002.

Appendix B

year	month	day	time	mN	m1	# stns	lat	long	depth	Location
2002	2	11	11:41	3.8MN	3.21	15	46.06	-73.46	10	6 km N from Joliette, Que. Felt.
2002	2	24	21:38	3.1MN	2.41	*	45.29	75.17	18	38 km SE from Buckingham, Que. Felt.
2002	4	1	16:05	3.1MN	2.55	*	46.3	-75.76	18	19 km SE from Maniwaki, Que. Felt.
2002	4	20	10:50	5.5MN	4.61	31	44.53	-73.73	18	Plattsburgh, N.Y., U.S. Felt.
2002	4	20	11:08	3.0MN	3.50	5	44.53	-73.7	18	Plattsburgh, N.Y. Aftershock.
2002	4	20	11:45	3.1MN	2.62	*	44.58	-73.69	18	Plattsburgh, N.Y. Aftershock.
2002	4	25	12:51	3.1MN	2.47	*	46.22	72.73	18	17 km E from Louiseville, Que.
2002	5	3	17:07	2.7MN	2.16	*	46.11	75.02	18	60 km W from Ste-Agathe-des-Monts, Que.
2003	5	9	15:56	2.6MN			46.9	75.83	18	47 km NW from MONT-LAURIER, QUE.
2002	5	24	23:45	3.5MN	3.00	11	44.5	-73.68	10	Northern New York. Aftershock.
2002	6	1	11:35	3.2MN	2.33	6	45.59	-73.86	18	7 km W from Laval, Que. Felt.
2002	6	5	20:17	4.5MN	3.63	37	52.85	-74.35	5	230 km E from Radisson (LG-2), Que.
2002	6	25	13:40	3.4MN	2.95	5	44.53	-73.67	10	Plattsburgh, N.Y., U.S. Felt. Aftershock
2002	8	17	5:53	3.8MN	3.12	13	47.33	-70.51	13.3	10 km S from Baie-Saint-Paul, Que. Felt.
2002	8	24	6:47	3.1MN	2.94	5	47.43	-74.88	18	57 km S from Parent, Que.
2002	9	7	21:27	3.7MN	2.92	11	46.96	-76.29	18	65 km N from Maniwaki, Que. Felt.
2002	11	7	16:55	3.0MN			44.07	-77.44	5	12 km SW from BELLEVILLE, ONT.
2003	1	2	15:46	2.8MN			46.3	-74.56	18	NW from Ste-Agathe-des-Monts, Que.
2003	1	9	16:18	2.9MN			45.59	-74.46	18	SW from LACHUTE, QUE.
2003	1	21	10:29	2.9MN			43.76	-77.97	18	SE from Port Hope, Ont.
2003	1	28	16:52	3.0MN			45.31	-74.92	18	NW from Cornwall, Ont.
2003	2	9	16:18	3.3MN			46.54	-75.2	18	E from Mont-Laurier, Que. Felt.
2003	2	25	15:11	2.5MN			45.52	-75.36	18	SE from Buckingham, Que. Felt.
2003	2	25	16:24	3.0MN			46.65	-76.57	18	NW from MANIWAKI, QUE.
2003	3	14	10:33	3.1MN	2.66	9	45.66	-77.36	18	SW from Pembroke, Ont. Felt.
2003	4	8	15:06	3.7MN	2.92	9	44.62	-74.37	11.9	SE from CORNWALL, ON.
2003	4	17	15:54	2.9MN			46.08	-75.69	18	SE from MANIWAKI, QUE.
2003	6	13	11:34	4.1MN	3.34	27	47.7	-70.09	11.1	CHARLEVOIX SEISMIC ZONE, QUE.
2003	6	30	19:21	3.6MN	3.16	3	41.8	-81.27	18	Shore of Lake Erie.
2003	8	5	1:57	2.8MN			46.81	78.94	18	68 km NE from NORTH BAY, ONT.
2003	8	20	1:58	3.5MN	2.91	13	46.01	-74.95	18	NW from Hawkesbury, Ont.
2003	9	19	17:22	3.3MN	2.88	5	45.79	-74.85	18	NE from BUCKINGHAM, Que.
2003	10	12	8:26	4.5MN	3.58	30	47.01	-76.36	18	NW from MANIWAKI, QUE.
2003	11	4	6:58	2.6MN			46.37	-77.47	18	N from PETAWAWA, ONT.
2003	11	22	14:41	2.6MN			45.56	-76.44	18	N from BRAESIDE, ONT.
2003	11	30	3:30	2.6MN			44.06	-77.43	18	S from BELLEVILLE, ONT.
2003	12	7	18:59	2.6MN	2.21	3	45.13	-75.22	18	N from IROQUOIS, ONT.
2003	12	11	23:27	2.8MN			46.7	76.41	18	49 km NW from MANIWAKI, QUE.
2004	1	1	10:10	2.5MN			46.57	76.29	18	32 km NW from MANIWAKI, QUE.
2004	1	18	7:56	2.6MN			47.36	76.01	18	98 km NW from MONT-LAURIER, QUE.
2004	2	26	22:39	2.5MN			46.38	-76.95	18	59 km NE from PETAWAWA, ONT.
2004	3	5	13:31	2.6MN			46.42	-75.16	18	
2004	3	17	12:38	2.5MN			45.05	-75.66	18	17 km SW from Cornwall, Ont.
2004	3	17	22:01	2.8MN			44.92	-74.88	18	
2004	6	2	12:49	2.6MN			46.87	-77.22	18	88 km N from Deep River, ON
2004	6	16	6:31	3.1MN			42.79	-79.08	18	18 km SE from Port Colborne, ON
2004	6	23	23:28	2.6MN			45.95	-74.86	18	28 km SW from Saint-Jovite, QC
2004	6	28	6:10	4.7MN	3.90	29	41.35	-89.03	18	Illinois, U.S.
2004	6	30	4:03	3.3MN			41.84	-81.19	18	Ohio, near Painesville
2004	7	22	13:10	3.1MN	2.35	7	46.54	-75.02	18	Felt in Sainte Veronique, Quebec
2004	8	4	23:55	3.8MN	3.29	18	43.68	-78.24	4	30 km S from Port Hope, ON. Felt.
2004	9	4	2:05	3.1MN	2.64	7	44.89	-74.92	4	20 km E from Morrisburg, ON. Felt.
2004	12	3	0:06	2.8MN	2.47	4	45.94	-74.88	18	29 km NE from Saint-Andre-Avellin,
2005	3	6	6:17	5.3MN	4.42	44	47.75	-69.73	13.3	CHARLEVOIX SEISMIC ZONE, QUE.

Appendix B: Table of events used in study. mN = Nuttli magnitude, m1 = empirical magnitude estimate, # stns = number of stations used in m1 estimate. Depth= estimated or assigned depth in km. *: m1 calculated by Atkinson (2004)